



## The CHRONOS mission: Capability for sub-hourly synoptic observations of carbon monoxide and methane to quantify emissions and transport of air pollution

5 David P. Edwards<sup>1</sup>, Helen M. Worden<sup>1</sup>, Doreen Neil<sup>2</sup>, Gene Francis<sup>1</sup>, Tim Valle<sup>3</sup>, and Avelino F. Arellano, Jr.<sup>4</sup>

<sup>1</sup>National Center for Atmospheric Research (NCAR), Boulder, CO, USA

<sup>2</sup>NASA Langley Research Center, Hampton, VA, USA

<sup>3</sup>Ball Aerospace, Boulder, CO, USA

10 <sup>4</sup>University of Arizona, Tucson, AZ, USA

*Correspondence to:* D. P. Edwards ([edwards@ucar.edu](mailto:edwards@ucar.edu))

15

### Abstract:

The CHRONOS space mission concept provides time-resolved abundance for emissions and transport studies of the highly variable and highly uncertain air pollutants carbon monoxide and methane, with sub-hourly revisit rate at fine (~ 4 km) horizontal spatial resolution across a North American domain. CHRONOS can provide complete synoptic air pollution maps (“snapshots”) of the continental domain with fewer than 10 minutes of observations. This rapid mapping enables visualization of air pollution transport simultaneously across the entire continent and enables a sentinel-like capability for monitoring evolving, or unanticipated, air pollution sources in multiple locations at the same time with high temporal resolution. CHRONOS uses a compact imaging gas filter correlation radiometer for these observations, with heritage from more than 17 years of scientific data and algorithm advances by the science teams for the MOPITT instrument on NASA’s Terra spacecraft in low Earth orbit. To achieve continental-scale sub-hourly sampling, the CHRONOS mission would be conducted from geostationary orbit, with the instrument hosted on a communications or meteorological platform. CHRONOS observations would contribute to an integrated observing system for atmospheric composition using surface, suborbital and satellite data with atmospheric chemistry models, as defined by the Committee on Earth Observing Satellites. Addressing the U.S. National Academy’s 2007 Decadal Survey direction to characterize diurnal changes in tropospheric composition, CHRONOS observations would find direct societal applications for air quality management and forecasting to protect public health.

35



## 1 Introduction

For the end of the current decade, geostationary Earth orbit (GEO) satellite missions for atmospheric composition are planned over North America, East Asia and Europe, with additional missions in formulation or proposed. Together, these present the possibility of a constellation of GEO platforms to achieve continuous, time-resolved, high-density, observations of continental domains for mapping pollutant sources and variability on diurnal and local scales with near-hemispheric coverage (CEOS, 2011). In addition to NASA's TEMPO mission (Zoogman, 2016), the ESA/EUMETSAT Sentinel 4 mission over Europe (GACS, 2009) and the Korean KARI MP-GEOSAT/GEMS mission over Asia (Lee et al., 2010), will provide data products for ozone (O<sub>3</sub>), nitrogen dioxide (NO<sub>2</sub>), sulfur dioxide (SO<sub>2</sub>), formaldehyde (HCHO) and aerosol optical depth (AOD) several times per day with smaller than 10 km x 10 km spatial footprints.

This observational constellation will be further enhanced by current and upcoming low Earth orbit (LEO) missions with atmospheric composition measurement capability. These missions include OMI (Ozone Monitoring Instrument, Levelt et al., 2006), IASI (Infrared Atmospheric Sounding Interferometer, Clerbaux et al., 2009), CrIS (Cross-track Infrared Sounder, Gambacorta et al., 2014), OMPS (Ozone Mapping Profiler Suite, Flynn et al., 2014), and the ESA Sentinel-5 precursor mission, TROPOMI (Veefkind et al., 2012). The LEO assets allow for a transfer-standard between the GEO missions, filling gaps in the spatial coverage, enabling cross-calibration and validation, and potentially, combined data products. Such an integrated global observing system for atmospheric composition is key to abatement strategies for air quality as prescribed in international protocols and conventions (e.g., Barrie et al., 2004).

While these planned GEO measurements will provide new information on the diurnal evolution of emissions and chemical transformation of some important pollutants, they are missing observations of methane (CH<sub>4</sub>) and carbon monoxide (CO). As identified in CEOS (2011), these gases play key roles in atmospheric chemistry, air quality and climate. Pollution affecting air quality is a complex mixture of many compounds that was designated a Group 1 carcinogen by the World Health Organization (WHO) (Loomis et al., 2013) amidst rising concerns about increased mortality and economic costs. Outdoor air pollution causes pulmonary and cardiovascular diseases, lung cancer, and premature birth (Brunekreef and Holgate, 2002; Turner et al., 2015; Fann et al., 2012, Malley et al., 2017). Despite improvements in U.S. air quality in recent decades, present-day levels of air



pollution decrease average life expectancy by 0.7 years and contribute to 10% of the total deaths in highly polluted areas such as Los Angeles (Fann et al., 2012). In 2010, over 3% of U.S. preterm births were attributed to air pollution at an estimated cost exceeding \$5 billion (Trasande et al., 2016). To address the causes of air pollution effectively, decision makers need comprehensive measurements to quantify the full suite of pollutants, including CH<sub>4</sub> and CO, emitted from industrial, transport and energy sectors, as well as natural sources. CO, which allows detection of combustion-related emissions, serves as the reference for the emissions of many difficult-to-measure pollutants that impact air quality and climate. Wildfires, which emit both CO and CH<sub>4</sub>, are a particular concern in the Western U.S. (Abatzoglou and Williams, 2016), where burn areas have increased by a factor of 6 since 1970, with severe economic impacts (Westerling et al., 2006). CO and CH<sub>4</sub> emissions also have significant consequences for climate change, especially considering CH<sub>4</sub> pollution due to recent large increases in natural gas production (Pétron et al., 2012; Miller et al., 2013) and potential new CH<sub>4</sub> releases from thawing permafrost (Ciais, 2013).

After air pollutants are emitted, they are transported vertically and horizontally in the atmosphere and can have a significant impact on local air quality and human health at locations near the sources and also downwind. Distinguishing the relative contributions of local and non-local pollution sources has emerged as a fundamental challenge for air quality management in the U.S. (NRC, 2004). Because CO has a medium lifetime (weeks to months), it can be transported globally, but does not become evenly mixed in the troposphere. This moderate lifetime makes CO an ideal tracer of combustion-related air pollution (e.g., Edwards et al., 2004; 2006).

The CHRONOS mission is motivated by these fundamental questions regarding the emissions and transport of air pollutants. The CHRONOS gas filter correlation radiometry (GFCR) measurement technique for multi-spectral CO builds on 17 years of observations from the NASA Terra satellite Measurements of Pollution in the Troposphere (MOPITT) instrument (Drummond et al., 2010, Worden et al., 2013), in addition to experience in LEO column CH<sub>4</sub> retrievals from SCIAMACHY (Frankenberg et al., 2005; 2011) and GOSAT (Morino et al., 2011, Schepers et al., 2012). The CHRONOS temporal resolution (sub-hourly), and spatial resolution (nominally 4 km × 4 km at the center of the domain), are required to capture the near surface trace gas variability, as concluded by modeling and data studies performed by the Geostationary Coastal & Air Pollution Events (GEO-CAPE) (Fishman et al., 2012) science team in response to the first Decadal Survey for Earth Science



and Applications (NRC, 2007). For CH<sub>4</sub>, the spatially and temporally dense CHRONOS measurements over the entire continental U.S. measurement domain would address the need for consistent assessments of CH<sub>4</sub> emissions at decision-relevant scales. For CO, proven multispectral retrieval techniques (Worden et al., 2010) increase the information on CO vertical distribution, and  
100 can identify vertical transport from one observation to the next. Thus, CHRONOS is capable of tracking pollutants from the surface where they are emitted, to where they degrade downwind air quality.

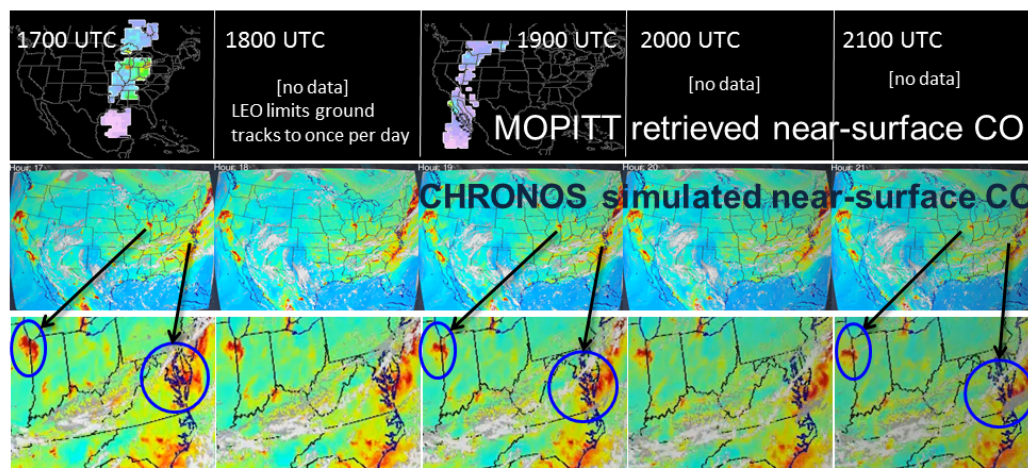
This paper describes the CHRONOS science, measurement technique, expected performance (precision and accuracy), retrieval vertical sensitivity and observing strategy. We then show how  
105 CHRONOS would complement observations from other current and planned satellite instruments, and conclude with a summary of CHRONOS features and advantages.

## 2 CHRONOS Science

### 2.1 CHRONOS Sub-hourly Synoptic Measurements with High Spatial Resolution

110 Advances in tropospheric remote sensing from LEO over the past decade have shown the potential of satellites to quantify the sources, transport and distributions of the gases important for air quality and climate (NRC, 2007; Simmons et al., 2016). LEO data provide valuable knowledge on continental to global-scale pollution, but their spatial and temporal resolution, sparseness of coverage, and often large uncertainties for individual trace gas observations, have so far limited their use in understanding  
115 air pollution sources and distributions on local to regional spatial scales (Figures 1 and 2).

The importance of hourly time resolution for capturing the diurnal evolution of pollution transport is shown in Figure 1, which compares current MOPITT measurement sampling to that which would be obtained from CHRONOS over the continental U.S.



120 **Figure 1:** Comparison of MOPITT and CHRONOS spatiotemporal coverage over a 5-hour period. The top panels show MOPITT retrievals of near-surface CO for Aug. 1, 2006 with pink colors indicating low CO (~ 60 ppbV) and green to red indicating higher values (200 – 300 ppbV). The middle and bottom panels show a simulation of CHRONOS observations using WRF-Chem (Grell et al., 2005) at 4 km horizontal resolution for the same date with blue colors indicating low CO (~60 ppbV), red colors indicating high CO (~300 ppbV) and light grey indicating clouds. Circled areas in the zoomed bottom panels provide detailed examples of changes in CO concentrations over the 5-hour period with pollution from Chicago moving to the south and clouds moving east over the Washington DC area.

130 Understanding the rapidly changing tropospheric state and critical processes that are episodic or have diurnal timescales, such as traffic emissions, forest fire intensity, meteorology and changes in the planetary boundary layer (PBL) height, requires temporal resolution that is better than once a day (Fishman et al., 2012). Accurate prediction of air quality requires an observing framework for atmospheric composition similar to that for weather forecasting, where instruments in GEO are  
135 essential components of the integrated observing system and complement existing LEO, suborbital, and surface assets and modeling capability. As such, CHRONOS in GEO addresses the need for sub-hourly vertical and horizontal transport information for “chemical weather” prediction.

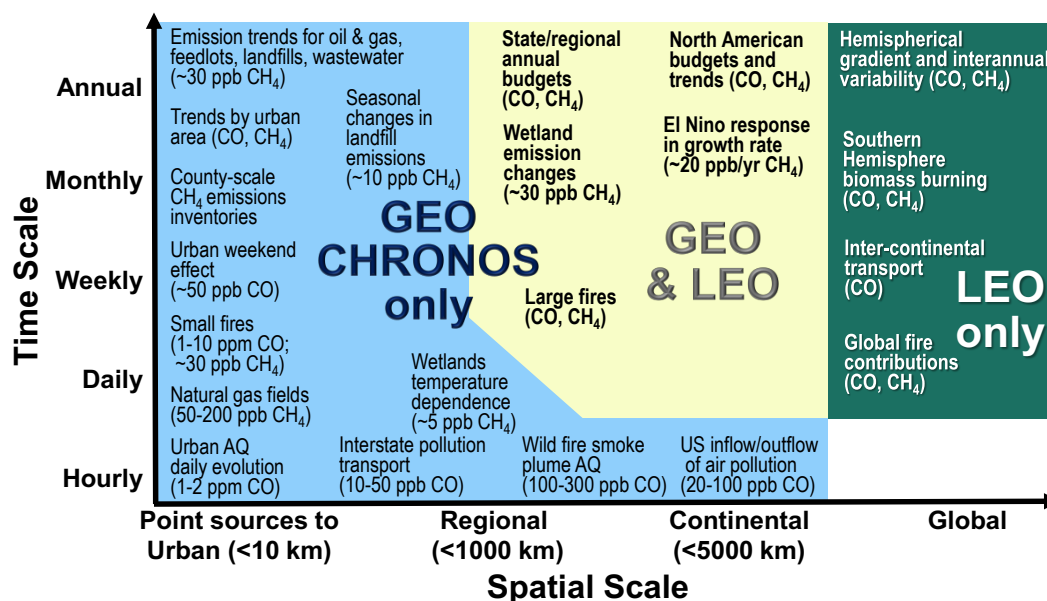


**Figure 2:** CHRONOS' sub-hourly observations would provide access to the fine temporal and fine spatial scales of CH<sub>4</sub> and CO processes for understanding the emissions and transport of air pollution for air quality, climate, and energy management applications. Estimated abundances are for process contributions above background levels.

## 2.2 The CHRONOS Science Objectives

CHRONOS focuses on two interrelated science objectives: emissions of highly variable and poorly quantified air pollutants, and air pollution transport across North America. Significant scientific advances in understanding these air pollutant emissions and transport processes are expected to lead to improvements in chemical transport model predictability on both regional and global scales.

**Objective 1 – Emissions:** *Quantify the temporal and spatial variations of CH<sub>4</sub> and CO emissions for air quality, climate, and energy decision making.*

Large uncertainties and conflicting estimates exist in current CO and CH<sub>4</sub> emissions. Aircraft data show National Emission Inventory (NEI) (U.S. EPA, 2011) CO emissions are too high by a factor of 3 in the summer (Hudman et al., 2008; Miller et al., 2008). Satellite data, including MOPITT, indicate large seasonal changes in CO emissions with a maximum in winter and minimum in summer (Kopacz





155 et al., 2010), that are currently absent from the NEI, and show fire emissions that are too low by as  
much as 30% (Pechony et al., 2013). Measurements of CH<sub>4</sub> from surface and aircraft observations  
imply that the EPA 2009 emission inventory is too low, by about a factor of 2, due to large  
uncertainties from fossil fuel production (coal and natural gas fields, especially in the Western States  
and Canadian tar sands), transportation, agriculture, wetlands, and thawing permafrost in Canada  
160 (Katzenstein et al., 2003; Xiao et al., 2008; Kort et al., 2008; Pétron et al., 2012; Miller et al., 2013;  
Pechony et al., 2013; Schwietzke et al., 2016). In particular, for natural gas production, recent studies  
present conflicting results. Karion et al. (2013) showed ~6–12% CH<sub>4</sub> leakage from gas and oil  
production fields in Uintah County, Utah, using airborne measurements, while Allen et al. (2013)  
found less than 1% leakage at 190 U.S. natural gas sites using emissions activity estimates. Recent  
165 research identified sensor issues in the surface measurements used by natural gas companies often  
causing under-estimated emissions (Howard et al., 2015). These observational inconsistencies can be  
resolved by comprehensive measurements that are temporally and spatially dense.

CO observations also serve as proxy for other pollutant emissions. Emissions of other combustion  
pollutants that are important to air quality and climate are frequently correlated with CO emissions,  
170 including other ozone and aerosol precursors (Edwards et al., 2004; Massie et al., 2006; Zhang et al.,  
2008; Bian et al., 2010). As a result, the emission inputs to chemical transport models for many  
combustion-related species are specified by ratios referenced to CO. Carbon monoxide serves as a  
proxy for anthropogenic carbon dioxide (CO<sub>2</sub>) (Palmer et al., 2006; Worden et al., 2012; Silva et al.,  
2013) and black carbon (BC) sources (Arellano et al., 2010). CH<sub>4</sub> correlations with CO distinguish  
175 CH<sub>4</sub> from fires (Worden et al., 2013). Assimilation of CHRONOS data into regional scale chemical  
transport models would leverage inter-species constraints to allow the emissions and distributions of  
correlated species to be inferred using CHRONOS measurements (e.g., Gaubert et al., 2016).

**Objective 2 – Transport:** *Track rapidly changing vertical and horizontal atmospheric pollution  
transport to determine near-surface air quality at urban to continental spatial scales, and at diurnal  
180 to monthly temporal scales.*

Source attribution for local and transported pollution is an important step toward attaining air quality  
standards (NRC, 2004). Understanding the production of air pollution requires knowledge of ozone  
and aerosol precursor emissions (CO and CH<sub>4</sub> among them), and the transport of both precursors and  
other air quality pollutants (for example, using CO as a tracer). Air pollution crosses international and



185 state boundaries to impact downwind cities, national parks, and wilderness areas. The Cross-State Air  
Pollution Rule (U.S. EPA, 2011) requires 23 states to reduce emissions in order to meet air quality  
standards in downwind states. Considerable international efforts are directed toward understanding  
intercontinental transport of air pollution (Galmarini et al., 2017). CHRONOS' multispectral  
retrievals of CO would provide the vertical sensitivity to determine transport out of the PBL, into the  
190 free troposphere, and the vertical descent back to the surface at some distance downwind. This new  
CHRONOS information would allow state and local air quality managers to quantify interstate  
pollution, along with intermittent sources such as fires that affect the ability of urban areas to meet  
air quality standards.

The time and space scales of CHRONOS measurements are designed to be similar to the scales of  
195 models for regional air quality applications, leading to improvements in process representation. From  
observing system simulation experiments (OSSEs), we have demonstrated that data assimilation of  
simulated CHRONOS multispectral observations of CO significantly improves comparisons with the  
“true” surface CO values at EPA surface monitoring sites (Edwards et al., 2009). Sub-hourly  
measurements of CO throughout the troposphere would allow for more frequent data assimilation  
200 updates than is currently possible, which, along with increased accuracy in surface CO knowledge,  
would dramatically improve the skill for air quality prediction. OSSEs also demonstrate that  
CHRONOS' CO measurements augment TEMPO's ozone measurement capability through joint  
ozone-CO data assimilation (Zoogman et al., 2014).

### 2.3 CHRONOS Measurements of CH<sub>4</sub> and CO

205 More than half of CH<sub>4</sub> emissions are anthropogenic, with contributions from fossil-fuel production,  
animal husbandry and waste management, while wetlands are the primary natural source  
(Bergamaschi et al., 2009). CH<sub>4</sub> has an atmospheric lifetime of 8–10 years, and exerts 86 times the  
global warming potential of CO<sub>2</sub> emissions on a 20-year timeframe (Myhre et al., 2013). The U.S. is  
presently the world's largest producer of natural gas (Breul et al., 2013). Production has increased  
210 20% since 2008, with a corresponding need to quantify how much CH<sub>4</sub> is released during extraction.  
Furthermore, CH<sub>4</sub> has an impact on air quality as a precursor to tropospheric ozone and aerosols  
through changes in hydroxyl radical (OH) (Shindell et al., 2009). CH<sub>4</sub> thus plays a pivotal role in  
both air quality and climate, and co-benefits to both air quality and climate may arise from reducing  
CH<sub>4</sub> emissions (West et al., 2006; Shindell et al., 2009; UNEP, 2011; Schneising et al., 2014).





215 CHRONOS' frequent (sub-hourly) CH<sub>4</sub> observations would provide the information needed to  
resolve discrepancies in CH<sub>4</sub> emissions at the county, decision-making, scale.

Dense data sampling improves the capability for constraining model emissions (e.g., Bousseret et al.,  
2016; Wecht et al., 2016a). Figure 3 shows a grid representing the CHRONOS spatial resolution  
overlaid on aircraft measurements taken during the FRAPPE-DISCOVER-AQ field campaign (Pfister  
220 et al., 2017) in the Colorado Front Range on Aug. 2, 2014. This indicates high CH<sub>4</sub> in areas of  
extensive oil and gas extraction and feedlot operations in Colorado (Greeley and Platteville), as  
compared to other urban and rural locations. By comparison, CH<sub>4</sub> concentrations during the 2015  
Aliso Canyon leak (Conley et al., 2016), over the Los Angeles basin were an order of magnitude  
higher than these Colorado oil and gas concentrations, and thus could have been quantified from space  
225 using CHRONOS CH<sub>4</sub> observations, had they been available. Recent studies have demonstrated the  
potential for using CO and CH<sub>4</sub> satellite data to constrain sources using adjoint and other inversion  
models (Bergamaschi et al., 2007; 2009; Meirink et al., 2008; Kopacz et al., 2009; 2010; Fortems-  
Cheiney et al., 2011; Pechony et al., 2013; Wecht et al., 2014b; Turner et al., 2015; Jacob et al., 2016).  
These studies also show that present ability to optimize emission estimates is limited by the sparse  
230 sampling of present measurements. CHRONOS would provide the data density and near-surface  
abundance information that are needed in adjoint inversions for CO and CH<sub>4</sub> emissions estimates with  
the spatial and temporal resolution necessary to understand emission inventory errors.

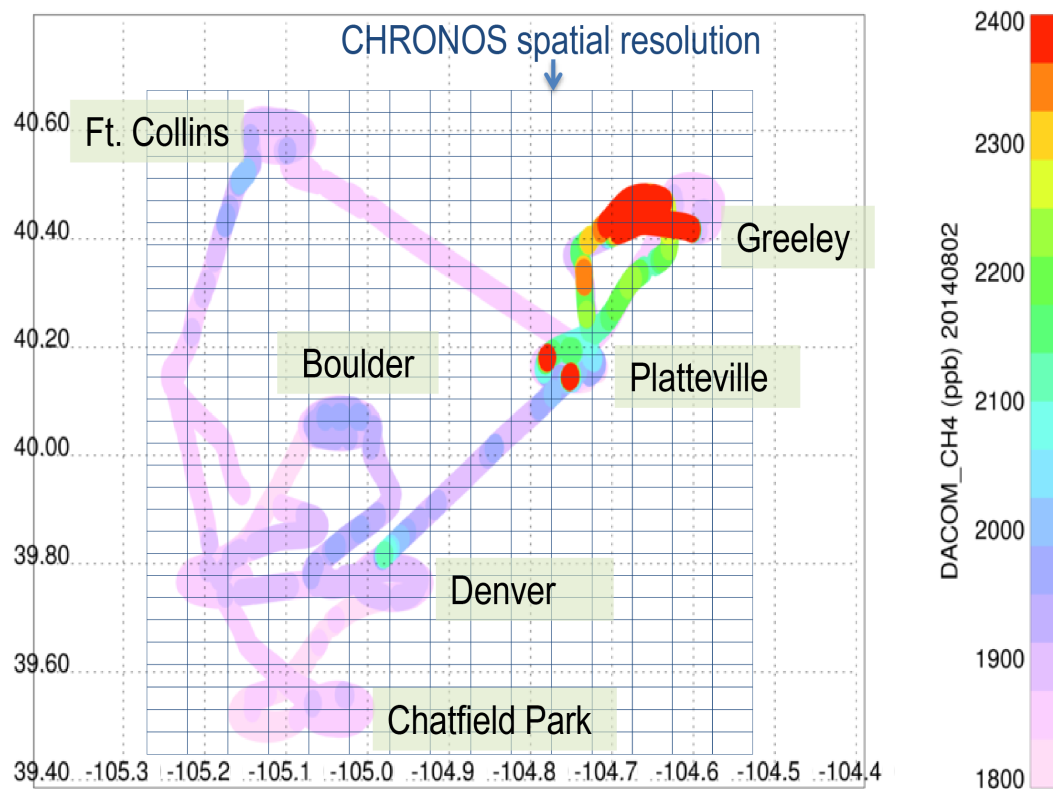


**Figure 3:** Aircraft in situ measurements of CH<sub>4</sub> from the FRAPPE-DISCOVER-AQ in the Colorado  
235 Front Range on Aug. 2, 2014. Vertical profiles were measured over cities, identified by spiral flight  
tracks. Note that the highest values of CH<sub>4</sub> are plotted last. Total column CH<sub>4</sub> computed from the  
vertical profiles is different by 4.9% between Ft. Collins and Greeley. CHRONOS spatial resolution  
is indicated by the overlaid grid, illustrating that CHRONOS column measurements would have the  
spatial resolution and precision to distinguish sub-hourly differences in city-scale CH<sub>4</sub> abundances  
240 from space. Data courtesy of Glenn Diskin, NASA.

Air quality criteria to protect public health were established for CO nine months before the Environmental Protection Agency was founded (U.S., 1970). Carbon monoxide is produced by combustion processes, including transportation, manufacturing, agricultural burning, and wildfires,



245 and by hydrocarbon oxidation. CO participates in the formation of ground level ozone; and, as the  
dominant sink for the main tropospheric oxidant, OH, CO plays a central role in determining the  
ability of the atmosphere to cleanse itself of pollutants (e.g., Holloway et al., 2000) and thus affects  
the lifetime of CH<sub>4</sub> (Myhre et al., 2013). The CO lifetime of ~2 months provides time for CO to be  
transported globally, yet is sufficiently short to show large contrasts between polluted air and the  
250 background atmosphere (Edwards et al., 2004). For these reasons, CO is one of the few mission-  
critical measurements in all aircraft campaigns of the NASA Global Tropospheric Chemistry Program  
(Fisher et al., 2010) and similar regional air pollution studies. CHRONOS would use the CO  
multispectral retrieval created by the MOPITT team providing enhanced sensitivity to near-surface  
CO concentrations (Worden et al., 2010; Deeter et al., 2013). This allows CO plumes near the surface  
255 to be distinguished from plumes in the free troposphere to quantify how sources of CO impact  
downwind regions (Huang et al., 2013). This approach is discussed in Section 5.

### 3 The Gas Correlation Filter Radiometry (GCFR) Measurement technique

#### 3.1 GCFR Concepts

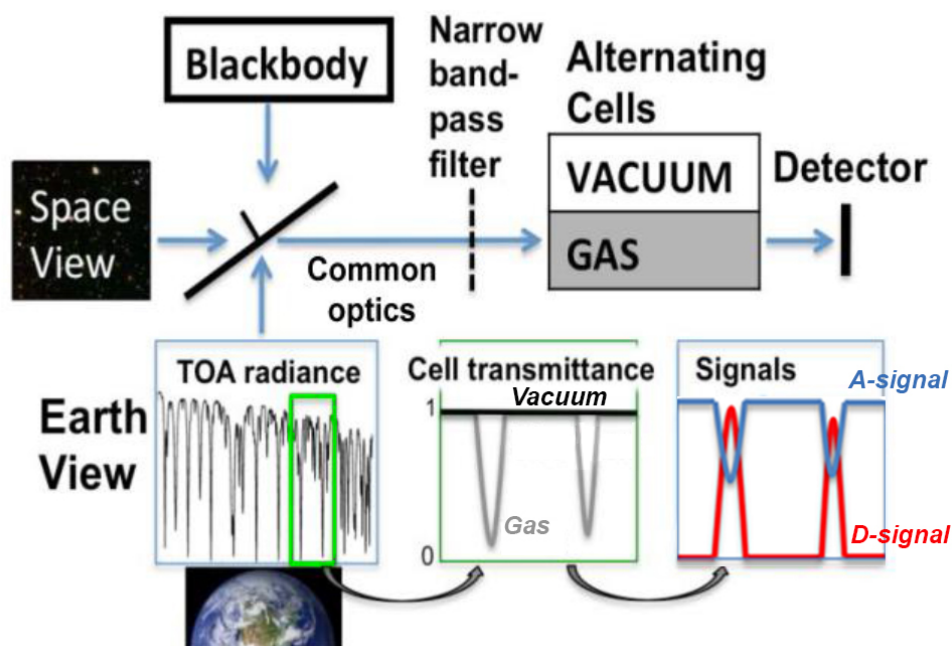
260 Gas filter correlation radiometry features extremely high spectral selectivity combined with high  
throughput to enable precise measurements of atmospheric trace constituents such as CH<sub>4</sub> and CO.  
Gas filter correlation radiometry (Action et al., 1972, Ludwig et al., 1973, Tolton and Drummond,  
1997) has been used for satellite remote sensing on Space Shuttle/MAPS (Reichle et al., 1999),  
UARS/ISAMS and HALOE (Rodgers et al., 1996; Russell et al., 1993), and Terra/MOPITT (Edwards  
265 et al., 1999; Drummond et al., 2010). The pioneering MAPS instrument used two detectors with  
careful electronic balancing on its four Space Shuttle flights to measure CO, and MOPITT uses length  
and pressure modulation of a single cell, rather than separate gas and vacuum cells, for its successful  
observations during more than 17 years in LEO. Correlation radiometers have thus proven rugged  
and reliable in space. The first Decadal Survey for Earth Science and Applications recommended “an  
270 IR correlation radiometer for CO mapping” and also stated that the “Combination of the near-IR and  
thermal-IR data will describe vertical CO, an excellent tracer of long-range transport of pollution  
(NRC, 2007).”

The GCFR technique is based on the concept that the near ideal filter for the spectral signal from a



particular molecule comes from the molecule itself. In the GFCR technique, shown schematically in  
275 Figure 4, the top-of-atmosphere (TOA) spectral radiance from each observed field of view (FOV)  
passes through an instrument cell containing the same gas as the atmospheric target gas being  
measured, either CO or CH<sub>4</sub> in the case of CHRONOS. The instrument cell uses the gas of interest as  
a highly selective filter to match narrow spectral features in the atmosphere. With known gas cell  
dimensions, gas content, temperature and pressure, this technique provides nearly perfect spectral  
280 knowledge. The GFCR method efficiently filters the target gas information from surrounding spectral  
interference, while simultaneously measuring and integrating the target spectra across the selected  
spectral bandpass, delivering a spectral response function that can be accurately calibrated because it  
is defined by the cell gas absorption. For these reasons, thorough GFCR instrument characterization  
is needed prior to launch, along with on-orbit radiometric calibration and measurements of cell  
285 parameters (Neil et al., 2010).

Idealized implementation of gas filter correlation radiometry requires viewing the same scene through  
the same optics with the same detector for each of two gas cells (one containing the gas of interest  
and the other containing a vacuum (or a gas with no spectral signature in the selected spectral region)).  
The goal is that the ratio of the spectral radiance viewed through the two cells is only a function of  
290 the target gas. Spatial misalignment of the two measurements could result in changes in the viewed  
surface reflectivity, and thus radiance changes in gas-vacuum cell difference. Temporal offsets could  
result in different atmospheric paths being captured because of target gas or cloud movement through  
the field of view. Changes in the instrument function between gas and vacuum views (different optics  
or detector) are equivalent to radiance errors. The CHRONOS implementation provides nearly  
295 simultaneous acquisition of the gas and vacuum cell signals through a common optical path, and  
minimizes ground co-registration errors between signal pairs. The displacement between a single  
paired gas/vacuum measurement is limited to  $\leq 5 \mu\text{rad}/60 \text{ msec}$  to ensure acceptable changes in ground  
pixel reflectance based on MOPITT experience (Deeter et al., 2011), and on simulated radiance errors  
using representative GEO spacecraft pointing data.



300

**Figure 4:** Simplified depiction of GFCR measurements to show how average (A) and difference (D) signals are generated from measurements through the vacuum (V) and gas (G) cells. Upwelling atmospheric radiance passes through a narrow bandpass filter, selected for the target gas spectral range, a target gas cell, and on to a detector pixel. For CHRONOS, within 60 msec, the atmospheric radiance passes through an identical bandpass filter, an identical reference vacuum cell, and falls on the same detector pixel.

305

In gas filter correlation radiometry, the relationship of the instrument analog signal and the actual spectrum must be interpreted using a forward atmospheric model and line-by-line spectral radiative transfer calculations (Pan et al., 1995). For instrument development, these calculations form the basis of the instrument spectral characteristics definition (bandpass and width for each target gas and spectral region), and quantify the instrument sensitivity to the target gas, the effects of signatures of non-target gases in the selected spectral region, and the effects of variations in the underlying surface. After launch, these calculations are a crucial part of the instrument model used in data retrieval.

315



### 3.2 Spectroscopy of CO and CH<sub>4</sub> and the CHRONOS Instrument Signals

Two CO spectral bands, the mid-wave infrared (MWIR) fundamental at 4.6  $\mu\text{m}$  (Figure 5) and the short-wave infrared (SWIR) overtone band at 2.3  $\mu\text{m}$  (Figure 6), are the only spectral regions that produce CO features easily distinguished from the surrounding spectra at wavelengths shorter than microwave, and thus are useful for passive remote sensing of tropospheric CO [e.g., Edwards et al., 1999; 2009]. Measurements in the MWIR band rely on thermal emission from the Earth's surface and atmosphere (that can be obtained both day and night), and relatively strong spectral features. Measurements in the MWIR are only sensitive to changes in lower atmosphere CO concentration when sufficient thermal contrast exists between the surface and near-surface atmosphere [Deeter et al., 2004]. Typically, MWIR signals are most sensitive to CO concentration changes in the mid-troposphere, where long-range pollution transport typically occurs. In contrast, measurements in the CO SWIR band rely on solar radiation reflected from the Earth's surface in daylight, with comparatively weak CO spectral features [Deeter et al., 2009]. Typically, the SWIR signal has almost uniform sensitivity to changes in the CO vertical profile, including information near the surface.

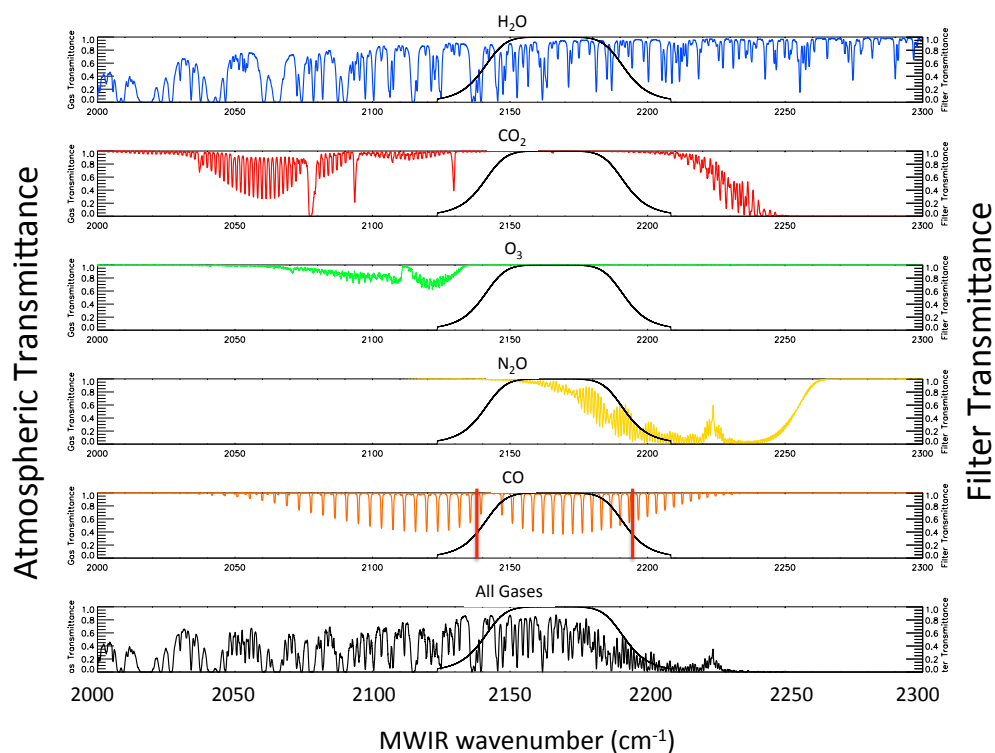






**Figure 5:** Atmospheric transmittance for primary trace gases in the MWIR vs. wavenumber. The CHRONOS filter transmission is indicated by smooth bandpass curves with solid red lines at filter half-power points. CHRONOS measures only CO in the MWIR.

335 Several spectral bands may be considered for retrieving CH<sub>4</sub>. Infrared measurements near 7.7 μm  
[e.g., Payne et al., 2009] generally lack sensitivity to near-surface CH<sub>4</sub>, similar to MWIR CO. Both  
SCIAMACHY (e.g., Frankenberg et al., 2005; 2011, Wecht et al., 2014b) and GOSAT (e.g., Morino  
et al., 2011, Schepers et al., 2012) have produced CH<sub>4</sub> data products using reflected sunlight in the  
SWIR to obtain a true total column. CHRONOS will also measure a 2.2 μm SWIR CH<sub>4</sub> band, shown  
340 in Figure 6.

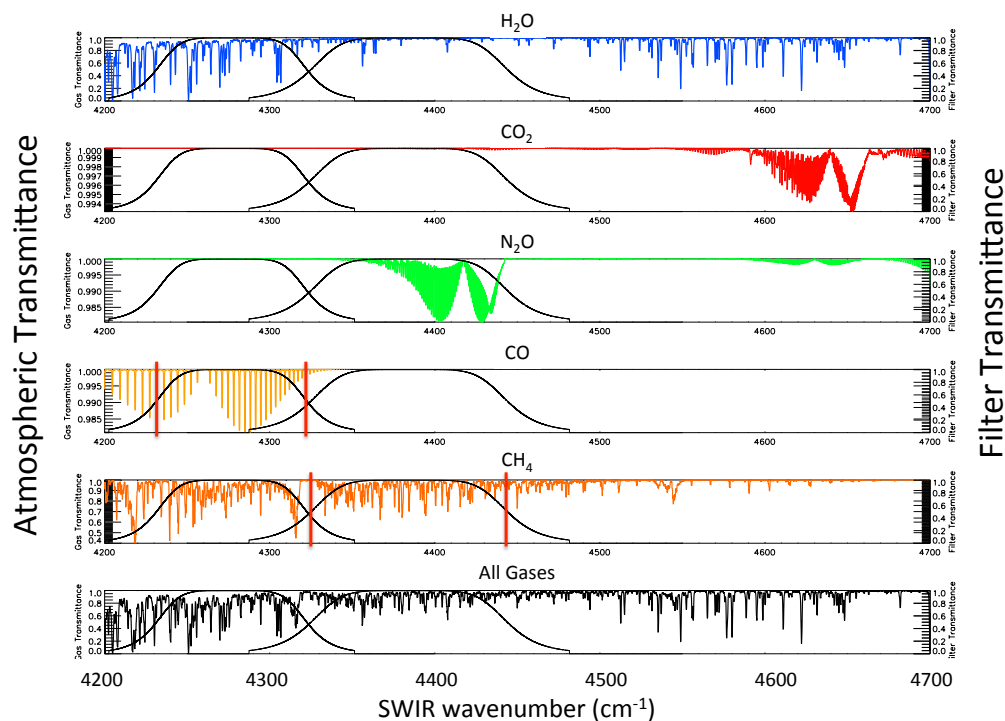


**Figure 6:** Atmospheric transmittance for primary trace gases in the SWIR vs. wavenumber. CHRONOS filter transmission is indicated by smooth bandpass curves with solid red lines at filter half-power points. CHRONOS measures both CO and CH<sub>4</sub> in the SWIR.



345 The GFCR instrument generates band-integrated spectral radiance measurements through alternate gas and vacuum cells, producing radiance pairs. As shown in Figure 4, the Difference (D-signal), constructed by differencing the gas and vacuum cell radiances, contains spectral contributions only from the target gas absorption line positions within the spectral passband. The Average (A-signal), the mean of the gas and vacuum cell radiances, has a spectral contribution that is low at the target gas  
350 line positions and high elsewhere. As such, the A-signal carries background information on the FOV scene characteristics. To first order, the ratio of the D-signal and A-signal,  $D/A$ , eliminates the background radiance term and reduces the impact of uncertainties associated with surface reflectance, interfering gases, aerosols and clouds.

The designated pressure in the instrument cell determines the width of the fill-gas spectral lines, and  
355 thus the effective spectral sampling resolution of the correlation filter. We note that the CHRONOS MWIR CO and SWIR CH<sub>4</sub> bands also contain water vapor (H<sub>2</sub>O) and nitrous oxide (N<sub>2</sub>O) absorption features (Figures 5 and 6). The gas correlation removes the absorption effects of these interfering gases for the D-signal. The interference of H<sub>2</sub>O and N<sub>2</sub>O in both the MWIR and SWIR channel A-signals is modeled in the forward model radiative transfer algorithm using analyzed H<sub>2</sub>O  
360 concentration fields from meteorological data and inferred N<sub>2</sub>O. N<sub>2</sub>O is a long-lived gas (~120 years) with predictable variability [Angelbratt et al., 2014].

### 3.3 Measurement Radiometric Accuracy and Precision

By using  $D/A$  radiance ratios, the GFCR technique is inherently less sensitive to radiance bias errors than spectrometer measurements. However, three primary sources of potential retrieval bias remain:  
365 surface albedo spectral variability, aerosol scattering, and water vapor errors in meteorological data, which are typically < 10% for N. America (Vey et al., 2010). Spectral variation in surface albedo proved to be a significant obstacle for MOPITT CH<sub>4</sub> retrievals (Pfister et al., 2005). This was because of the width and spectral location of the MOPITT passband, combined with changing scene albedo arising from LEO spacecraft motion during the acquisition of a single measurement (Deeter et al.,  
370 2011). For CHRONOS, the CH<sub>4</sub> passband has been optimized in both width and spectral location (Table 1) to mitigate these errors.

For a GFCR, the radiance precision needed to measure a change in column is given by  $\Delta D/A$ , for D and A defined above, where  $\Delta D$  is determined using the instrument sensitivity to the column change



375  $(\partial D / \partial \text{col})$  (Pan et al., 1995). To achieve the profile or column retrieval precision requirements, CHRONOS radiances will be averaged, after cloud detection, over ~3 minute intervals to perform retrievals, followed by averaging of these 3 minute retrievals to obtain full precision CO and CH<sub>4</sub> abundances in a single (~10 minute) data take.

380 **Table 1.** The multi-layer dielectric optical coatings on the CHRONOS gas cell windows define the center wavelength and bandpass. Each spectral coating and cell pressure is identified through modeling to provide the optimal measurement.

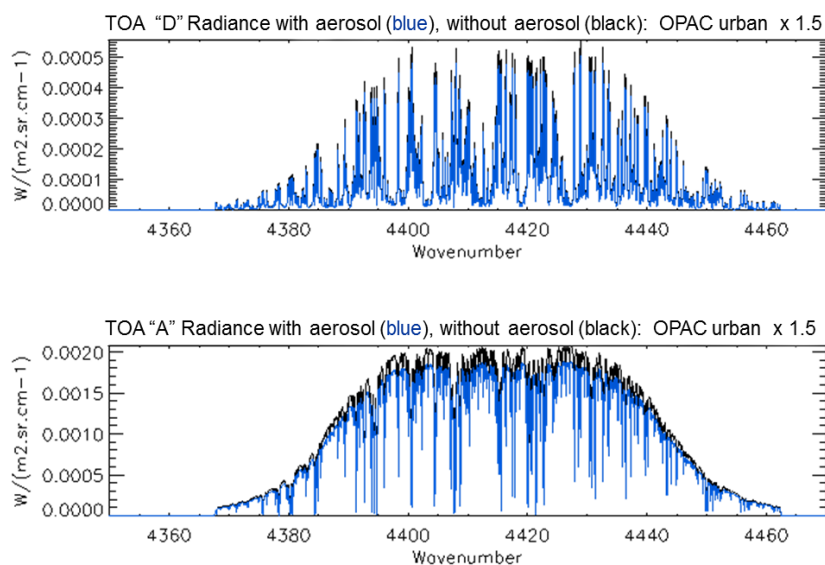
Cell	Gas	Center $\lambda$ ( $\mu\text{m}$ )	Pressure (hPa)	Band Pass ( $\mu\text{m}$ )	Band Pass ( $\text{cm}^{-1}$ )
1	CO	4.6	200	4.562 – 4.673	2140 - 2192
2	Vacuum	4.6	0	4.562 – 4.673	2140 - 2192
3	CO	4.6	800	4.562 – 4.673	2140 - 2192
4	CO	2.3	100	2.313 – 2.364	4230 - 4323
5	Vacuum	2.3	0	2.313 – 2.364	4230 - 4323
6	CH <sub>4</sub>	2.2	800	2.250 – 2.312	4325 - 4444
7	Vacuum	2.2	0	2.250 – 2.312	4325 - 4444
8	CH <sub>4</sub>	2.2	800	2.250 – 2.312	4325 - 4444

385 CO profile retrievals require 10% hourly precision to capture the fine-scale space and time variability of CO and quantify transient sources (Fishman et al., 2012; Emmons et al., 2009). Based on GEO-CAPE CH<sub>4</sub> emission OSSEs (Wecht et al., 2014a), monthly emissions estimates with <10% error on county-level spatial scales (~40 km x 40 km) require a daily precision on averaged retrievals of total column CH<sub>4</sub> <1%. CHRONOS will deploy two identical CH<sub>4</sub> channels with combined 0.7% precision that exceeds the GEO-CAPE requirement. This precision allows identification of CH<sub>4</sub> changes on daily scales, and verification of state and federal pollution reduction goals (Miller et al., 2013).

390 As discussed in Section 3.2, a major advantage of the GFCR measurement technique is the ability to eliminate any contaminating signal that is not spectrally correlated with the lines of the cell target gas. In the spectral regions utilized by CHRONOS, water vapor spectral lines are ubiquitous, and in the SWIR, the effects of aerosol must be considered. Figure 7 shows CHRONOS simulated A and D radiances for mid-latitude summer atmospheric conditions (Anderson et al., 1986), with and without



395 aerosol scattering. The VLIDORT radiative transfer model (Spurr, 2006) is used for modeling the  
aerosol scattering, and the OPAC (Optical Properties of Aerosols and Clouds) database (Hess et al.,  
1998) provides AOD adjusted to  $2.25 \mu\text{m}$ . The case shown in Figure 7 is for AOD that is 50% larger  
than the OPAC urban aerosol case. Based on the simulated retrievals we perform, 1% errors in total  
column correspond to 0.2% errors in D/A. The nominal urban aerosol loading considered in OPAC  
400 would lead to  $\sim 0.026\%$  errors in D/A, which translates to a  $\sim 0.13\%$  error in total column. Similar  
errors in D/A due to aerosol scattering are obtained for the CHRONOS  $2.3 \mu\text{m}$  CO channel, and can  
then be compared to MOPITT measurement errors in D/A that are around 1 to 2% for scenes with  
minimal geophysical noise. The insensitivity of D/A to aerosol scattering is found to hold for a large  
range of aerosol types and loading, with the largest errors (up to 0.3%) due to desert dust, consistent  
405 with Gloude-mans et al. (2008). Expected errors due to uncertainties in water vapor were also  
simulated using perturbations of the mid-latitude summer atmosphere and are  $< 1\%$  for CO and  $<$   
 $0.2\%$  for  $\text{CH}_4$ .



410 **Figure 7:** Forward model results with aerosol loading. Simulated radiance spectra for CHRONOS  
corresponding to TOA D (top panel) and A (bottom panel) signals with the CHRONOS  $\text{CH}_4$  SWIR  
channel bandpass applied. Simulations are for a mid-latitude summer atmosphere with solar zenith  
angle =  $0^\circ$ , satellite zenith angle =  $40^\circ$  and surface albedo = 0.2. Black lines represent the case without



aerosol scattering and blue lines show radiances with aerosol scattering for urban aerosols (AOD is 150% of the OPAC urban case). D/A is computed after integration over the bandpass and is changed  
 415 by -0.039% for the case with aerosols compared to without.

A summary of CHRONOS precision and accuracy requirements for column CO and CH<sub>4</sub> is given in Table 2. Validation activities for CHRONOS will use aircraft profiles from on-going flight programs, such as IAGOS (Nédélec et al., 2015) and existing ground data networks such as TCCON (Wunch et al., 2010) to detect biases in CO and CH<sub>4</sub> similar to the proven approach used for GOSAT and OCO-2 validation (Schepers et al., 2012).  
 420

**Table 2.** Expected precision and accuracy for CHRONOS.

Column Error Source	MWIR CO (night)	MWIR+SWIR CO (day)	SWIR CH <sub>4</sub> (day)
Precision requirement	<10%	<10%	<0.7%
MOPITT performance	5-15%	2-10%	n/a
Corresponding SNR (A/ΔD)	457	2499	3374
Radiometric bias	<0.1%	<0.1%	<0.1%
10% water vapor error	<0.7%	<0.7%	<0.15%
Albedo variation	negligible for MWIR CO band <sup>1</sup>	<0.06%	<0.1%
Urban aerosol loading	negligible in MWIR <sup>2</sup>	<0.03%	<0.13%

<sup>1</sup>(MWIR CO band is 0.11 μm wide; based on MOPITT experience, no significant errors due to albedo spectral variation)  
 425

<sup>2</sup>(e.g., Russell et al., 1999, Bohren and Huffman, 1983)

#### 4 The CHRONOS Instrument and Operation

The CHRONOS measurement domain, shown in Figure 8, extends over North America and includes adjacent oceans in order to observe pollution inflow and outflow using observations in the MWIR CO channels. In the SWIR channels, sunlight is mostly absorbed in the ocean, and no trace gas retrievals are expected over the ocean in the SWIR channels. The CHRONOS ground sample area varies gradually across the field of view due to curvature of the Earth as seen from GEO, with smaller than 4 km x 4 km (16 km<sup>2</sup>) nominal pixel area at the center of the domain, increasing to 19.3 km<sup>2</sup> at  
 430



435 the edge of the CONUS domain (e.g., Seattle). This spatial resolution enables emissions estimates at  
the U.S. county scale even for the smallest county in the continental U.S., New York County (i.e.,  
Manhattan), NY, which contains 3.5 CHRONOS pixels. The increase in pixel size toward northern  
latitudes is commensurate with the increasing scale of dominant emissions sources, such as large-  
440 scale wetlands in Canada (e.g., Pickett-Heaps et al., 2011). To account for these variations,  
CHRONOS Level 2 (individual retrieval) data will be re-gridded (Vijayaraghavan et al., 2008;  
Guizar-Sicairos et al., 2008) in Level 3 (gridded) data to facilitate user scientific analysis using  
standard tools.

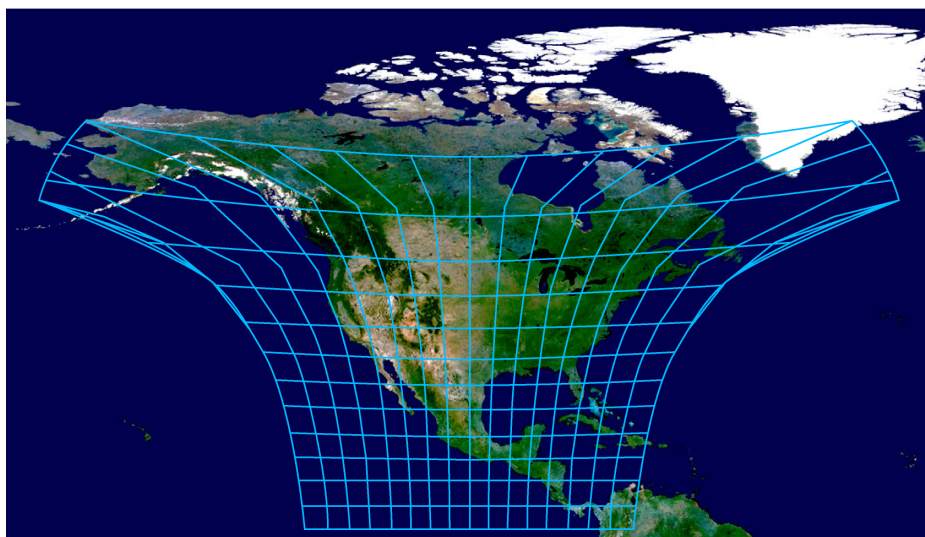


**Figure 8:** CHRONOS field of view from geostationary orbit at 100° W. Each grid cell above  
445 represents 125 x 125 pixels. All pixels are acquired with full precision within the ~10 minute  
CHRONOS data acquisition.

The CHRONOS GFCR is a staring infrared 2-D camera with a continuously rotating wheel that  
houses gas and vacuum cells which sequentially pass through the optical path. Figure 9 depicts the  
450 instrument, which comprises optomechanical, calibration, focal plane, thermal, and control  
electronics subsystems. Within the optomechanical subsystem, the gas cell filter wheel assembly  
contains cells as specified in Table 1. A selection mirror determines the source of the input radiance

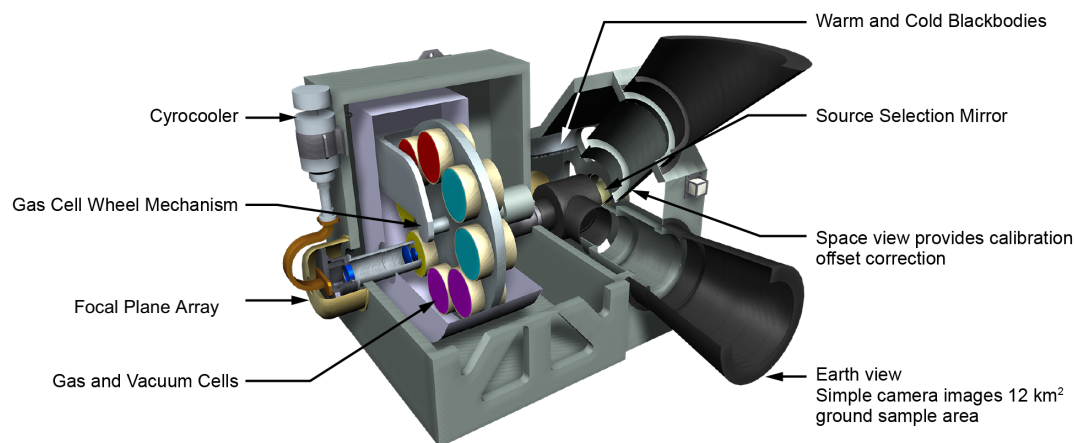




being filtered by the cells and imaged by the optics (Earth view, on-board calibration subsystem, a deep space view, and a blocked or closed position).

455 CHRONOS uses an all-digital cryogenically cooled HgCdTe large area focal plane array to detect the spectral radiance. The CHRONOS instrument has been designed around commercially available, space proven, radiation-hardened large format focal plane arrays (e.g., flown on India's Chandrayaan-1 mission/NASA Moon Mineralogy Mapper [Green et al., 2011], DOD's CHIRP experiment [Levi et al., 2011], and NASA's Near Infrared Camera on the James Webb Space Telescope [Garnett et al., 2004]). Low dark current ( $6.2 \times 10^9$  e-/cm<sup>2</sup>-s at 110 K), low readout noise (high gain: 40 e- rms; low gain: 200 e- rms), high, stable quantum efficiency (0.7 at 2.2, 2.3, and 4.6  $\mu$ m) and fast electronics are necessary characteristics for this application. For a 2-D imager such as CHRONOS, the pixel format (presently 2048 x 2048) and the desired observational domain determine the single pixel ground sample area from geostationary orbit.

465 A small, high-reliability, space-proven cryocooler cools the focal plane array and a portion of the optics module. Instrument control electronics provide the functionality to receive communications (commands) from the host spacecraft, control the instrument, sequence the data collection operations, and ultimately send science data to the host for downlink.



470 **Figure 9:** The CHRONOS GFCR is a staring infrared camera with gas cell filters in the optical path. A source selection mirror determines the input to the system (Earth FOV, one of three onboard calibration sources, deep space, or closed). Optics image this source input onto a cryogenically cooled large area focal plane array.



475 Figure 10 shows the image collection timing between a gas cell and its physically adjacent paired  
vacuum cell on a continuously rotating wheel. When an unobscured FOV emerges as a cell rotates  
through the optical path, the focal plane collects an image of the entire physical domain using one of  
two integration times (corresponding to low gain and high gain). Multiple gains are necessary to  
image the high dynamic range across the entire FOV with the required signal-to-noise ratio (SNR).  
480 Only 60 msec later, the FOV of the next cell, (a vacuum cell in the case of Figure 10), is unobscured  
and the focal plane collects an image. The short 60 msec between images effectively freezes the scene,  
allowing the GFCR algorithm to process the pair cell and vacuum signals together without geometric  
corrections, and providing nearly simultaneous gas and vacuum cell views described in Section 3.1.  
Single frames of paired gas and vacuum cell signals, as described above, are continuously collected  
485 until a prescribed number of images have been collected for each gas/vacuum cell pair. All of the  
images are downlinked through the host spacecraft. In ground processing, the single frame Level 0  
(signal count) data are processed for image registration and radiance calibration before being co-  
added to build up the required signal to noise ratio for the Level 1 (radiance) measurement at each  
location (pixel). The full data collection sequence includes calibration views, the full Earth view  
490 image collection outlined above for both low and high gains, followed again by calibration. The  
required SNRs for all channels are achieved in 9.7 minutes of measurement time. The CHRONOS  
gas cell filter wheel rotates continuously, and data may be obtained continuously, for up to 6 full-  
precision data takes per hour. Parameter tables can be uploaded to alter this sequence, or command  
additional data collects as necessary.

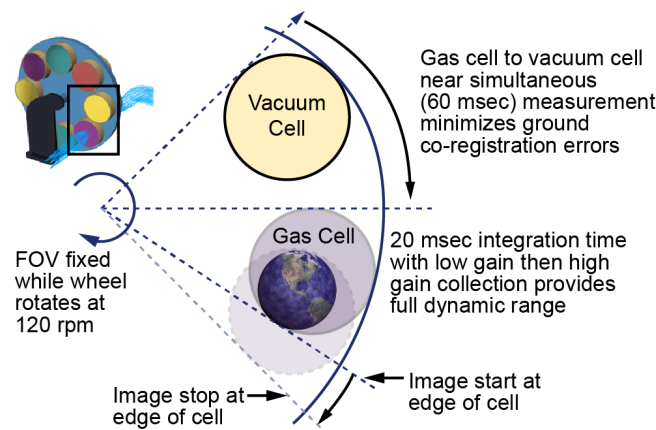




**Figure 10:** CHRONOS' eight gas cells are mounted in a continuously spinning mechanism wherein each cell in sequence exposes an unobscured Earth FOV as defined in Figure 8. A single frame image is collected with a prescribed integration time. Single frames are continuously collected and downlinked via the host spacecraft. In ground processing the ensemble of single frames are co-added to achieve the required signal to noise ratios for each measurement.

CHRONOS cloud detection will follow the MOPITT algorithm approach, which uses the MWIR A-Signals as the primary test for the presence of cloud, based on observed brightness temperature (Warner et al., 2001). In the case of MOPITT operation, cloud flags are then verified with the Moderate Resolution Imaging Spectroradiometer (Terra/MODIS) cloud data products, when available. Using a similar approach, CHRONOS will use the GOES-R Advanced Baseline Imager (ABI) cloud mask (Heidinger, 2011) to verify cloud detection. Cloud movement is assumed negligible during a 60 msec frame measurement. MOPITT retrieval experience shows that the GFCR technique can tolerate up to ~5% cloud contamination and still treat the pixel as cloud-free (Warner et al., 2001). Combined with CHRONOS' sub-hourly revisit, the small nominal ground sample area increases the probability of obtaining cloud-free pixels in regions of broken cloud. This is an advantage compared to observations from LEO where a cloud-free scene may not be encountered at a given location over several days. Figure 11 shows OSSE results for simulated CHRONOS observations over a 2-week summer period. This study indicates that 70–75% of 4 km x 4 km pixels can be treated as cloud-free in the West and Central U.S. and 60–65% in the East U.S.

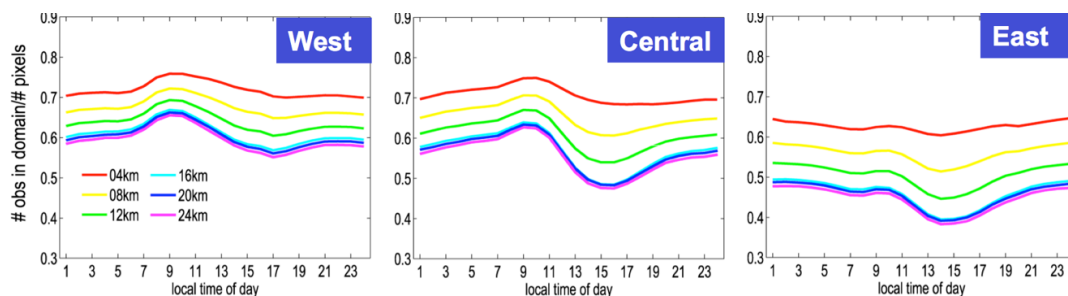


**Figure 11:** CONUS cloud statistics from OSSE results for 15-30 July 2006 using a high spatial resolution WRF-Chem run and a GFCR instrument with allowable pixel cloud fraction set at 3%. For



520 different geographical regions, the fraction of cloud-free scenes is plotted for different assumed pixel sizes; red represents the CHRONOS 4 km x 4 km pixels. Clouds are defined by 4-km grid integrated total hydrometeors  $> 10^{-8}$  kg/kg.

After cloud detection, the retrieval algorithm accesses current best meteorological analysis data for surface pressure and temperature, atmospheric temperature and water vapor profiles to include in the  
525 forward model radiance calculation. Optimal estimation (Rodgers, 2000) is then used to convert Level 1 TOA radiances to Level 2 vertical trace gas distributions.

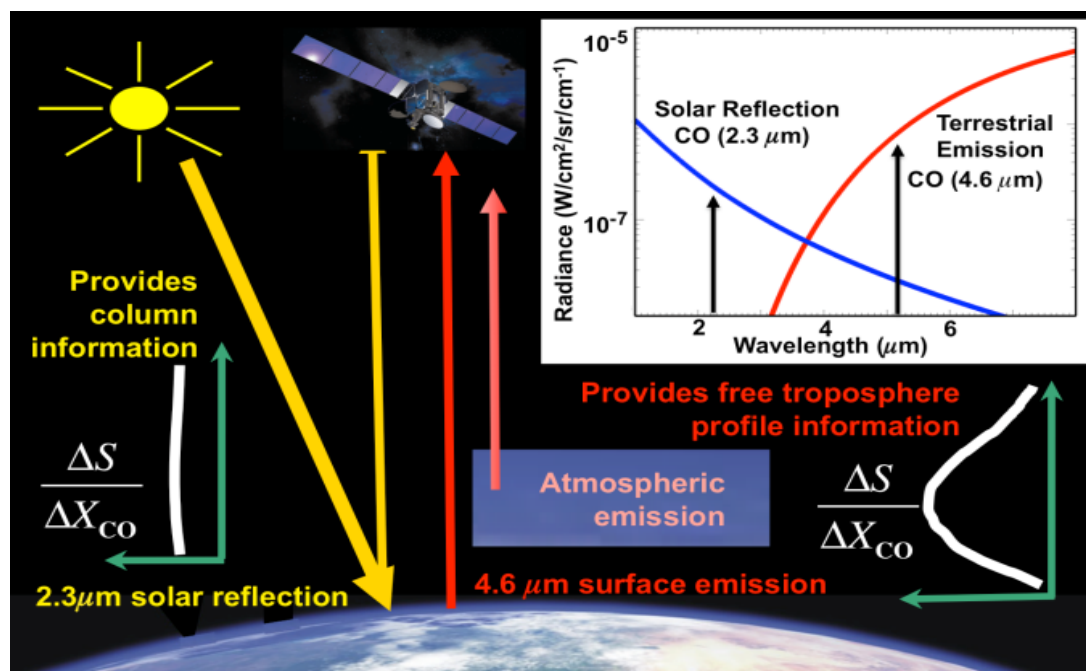
## 5 Characterization of CHRONOS CO and CH<sub>4</sub> Retrievals

### 5.1 Multi-spectral CO Measurements and Vertical Profile Information

530 CHRONOS CO measurements use MWIR thermal emission (day and night), with sensitivity to free tropospheric CO, and SWIR solar reflection (day), with sensitivity to total column CO. These measurements are combined in a multispectral retrieval to obtain vertical profiles of CO abundance, Figure 12. Following MOPITT retrieval algorithms, CHRONOS will employ the optimal estimation methods of Rodgers (2000), which provide an averaging kernel (AK) that represents the sensitivity  
535 of the retrieval to the abundance of the target trace gas in each retrieval pressure layer. Degrees of freedom for signal (DFS) in the retrieval are computed from the trace of the AK, and provide a measure of the independent profile information available. DFS values are  $\sim 1.5$  to 2 for retrievals using only MWIR channels with CO gas cells at two different pressures, while a column retrieval with the SWIR channel alone has at most a DFS of 1. The CHRONOS multispectral retrievals have DFS  
540 values typically  $> 2$ . Figure 13 shows CO retrieval results from MOPITT that compare the sensitivity of MWIR-only, SWIR-only and multispectral retrievals. We note that MOPITT retrievals would have higher values of DFS without the presence of geophysical noise in MOPITT observations (Deeter et al., 2011). Geophysical noise is introduced by changes in the FOV surface albedo due to LEO spacecraft motion during the time taken for MOPITT signal acquisition. The CHRONOS stationary  
545 FOV and single frame integration time of 20 msec mitigates this source of noise. Multispectral CO retrievals from MOPITT have demonstrated the improvements in sensitivity to surface layer CO abundance (Worden et al., 2010), have been validated (Deeter et al., 2011; 2013), and used in many studies to distinguish surface pollution emissions from transported plumes (e.g., Worden et al., 2012;



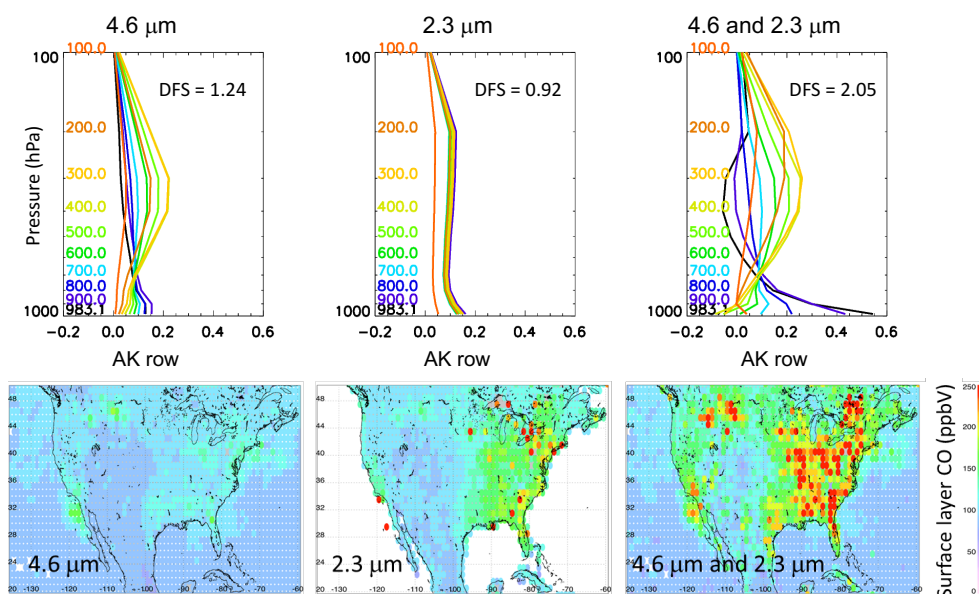
Jiang et al., 2013; 2015; He et al., 2013; Silva et al., 2013; Worden et al., 2013; Huang et al., 2013;  
 550 Anderson et al., 2014; Bloom et al., 2015). The CHRONOS multispectral retrievals would extend the  
 MOPITT record of vertical layers of CO over North America when MOPITT is finally  
 decommissioned, since MOPITT is the only satellite mission to demonstrate multispectral trace gas  
 retrievals from a single space-based instrument. The multispectral retrieval approach for CO allows  
 for up to 3 DFS, which is a practical upper limit on CO vertical information based on atmospheric  
 555 radiative transfer. As has been demonstrated by other on-orbit sensors measuring CO, an instrument  
 design with more gas cells, or a spectrometer with arbitrarily fine spectral resolution (George et al.,  
 2009), does not produce retrievals with greater DFS. Thus, CHRONOS would produce the maximum  
 vertical information possible for CO with a passive sensor.



560 **Figure 12:** Physics of CHRONOS and MOPITT multispectral measurements. In the SWIR at 2.2 and  
 2.3  $\mu\text{m}$ , measurement signals rely on daytime reflected solar radiation and weak spectral features.  
 Changes in  $\text{CH}_4$  and CO mixing ratios,  $\Delta X$ , produce uniform signal sensitivity,  $\Delta S$ , throughout the  
 vertical profile, including near the surface. In the MWIR at 4.6  $\mu\text{m}$ , signal sensitivity is greatest in  
 the middle troposphere, except in cases of high thermal contrast between the surface and the lowest  
 565 atmospheric layers. CHRONOS  $\text{CH}_4$  SWIR retrievals use the solar reflected radiance to provide a



true total column, and CO multispectral retrievals combine the SWIR and MWIR measurements to increase the sensitivity to near-surface CO. While this increased sensitivity varies depending on scene characteristics such as albedo, in many cases, it provides improved information to distinguish local air pollution emissions and transported plumes.



570

**Figure 13:** Comparison of surface layer CO for MOPITT MWIR (4.6 $\mu\text{m}$ ), SWIR (2.3  $\mu\text{m}$ ) and multispectral (MWIR and SWIR combined) retrievals for Aug. 2000. Top panels show representative averaging kernel (AK) rows, where line colors indicate the pressure layers given on the left side of the panels, for the three retrieval types (location at 30.72°N, 96.50°W). Bottom panels show maps of the surface layer CO abundance indicating how detailed information is obtained in the multispectral retrievals, but is absent in the single channel retrievals.

575

## 5.2 Retrieval Sensitivity to Near-Surface CH<sub>4</sub>

The vertical profiles of CH<sub>4</sub> are similarly characterized using the AK from optimal estimation retrievals (Rodgers, 2000). Radiative transfer modeling has been developed to compute weighting functions, i.e., radiance Jacobians integrated over the filter bandpass to assess the sensitivity to changes in the CH<sub>4</sub> column. Figure 14 shows an example of a simulated CHRONOS CH<sub>4</sub> weighting

580





function and corresponding AK (see caption for simulation assumptions). For the SWIR  
 measurements, the signal source is solar reflectance with a measurement sensitivity response that is  
 585 nearly uniform in the vertical, giving true total column information for CH<sub>4</sub> with DFS close to 1.

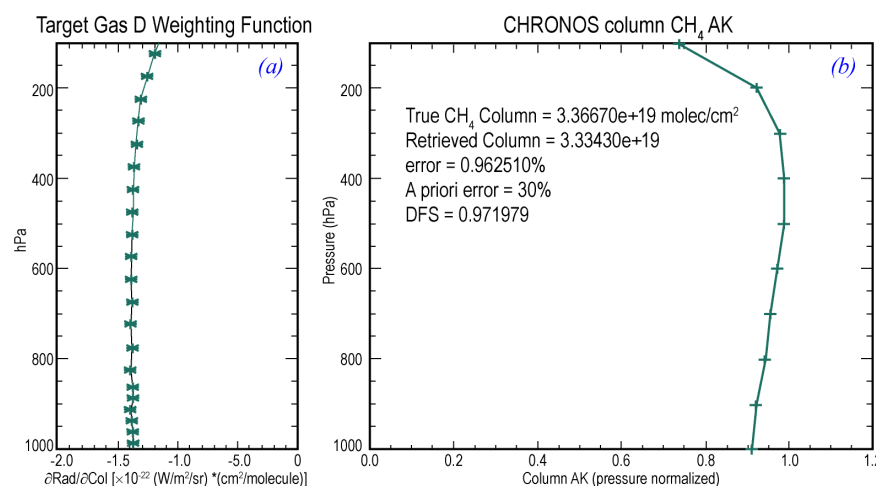


**Figure 14:** CHRONOS CH<sub>4</sub> D-signal weighting function and retrieval column AK. (a) Sensitivity of  
 the D-signal to changes in CH<sub>4</sub> column ( $\partial \text{Rad}(\mathbf{D}) / \partial \text{col}$ ) as a function of vertical pressure for a  
 standard mid-latitude summer atmosphere with albedo = 0.1, SZA = 0°, satellite ZA = 40°. (b) The  
 590 retrieval column averaging kernel from the corresponding D/A radiance ratio and Jacobian. This  
 assumes CHRONOS measurement precision and a priori covariance with 30% diagonal errors and  
 500 hPa correlation length, (retrieval was performed on a coarser pressure grid than the weighting  
 function calculations). Since the signal source is solar reflectance, the response is nearly uniform  
 vertically, giving true total column information for CH<sub>4</sub> with DFS close to 1.

595

The magnitude and shape of the column CH<sub>4</sub> AKs have only small variations with input atmospheric  
 parameters (such as temperature and water vapor) and input surface parameters such as albedo  
 (assuming non-zero albedo). However, there is a more significant dependence of the CH<sub>4</sub> AK on  
 parameters that depend on the total amount of CH<sub>4</sub> along the observation path, such as solar zenith  
 600 angle (SZA), satellite zenith angle and CH<sub>4</sub> abundance. Figure 15 shows how the sensitivity to CH<sub>4</sub>  
 in the lowest (near-surface) layer depends on SZA for A, D and D/A signals. While the A and D  
 signals both have reduced sensitivity with higher SZA, as expected for solar reflection radiances, the



D/A ratio sensitivity increases slightly, with relatively uniform response, for daylight hours. Figure 16 shows the dependence of CH<sub>4</sub> AKs on SZA and CH<sub>4</sub> total column, with sensitivity to surface CH<sub>4</sub> that increases with increasing values, especially for SZA, as expected from Figure 15.

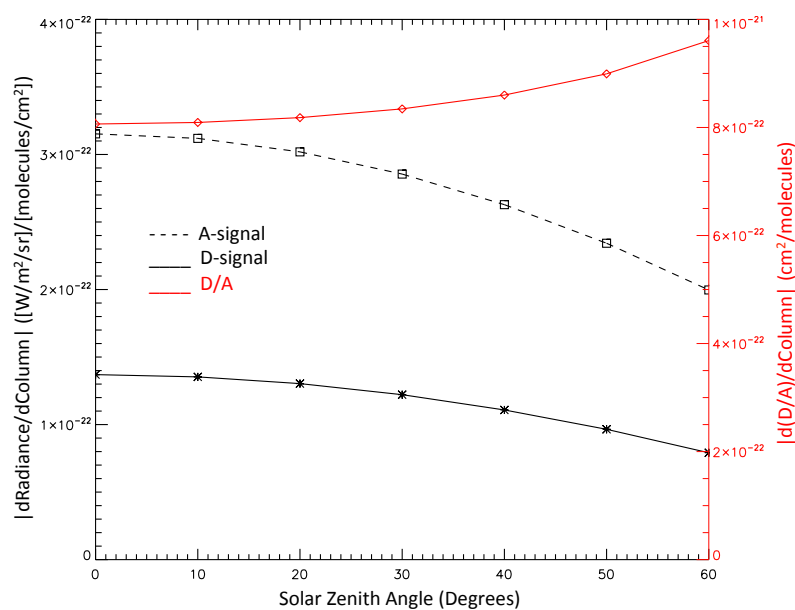


**Figure 15:** Variation of CHRONOS sensitivity to surface CH<sub>4</sub> with solar zenith angle (SZA). Absolute values for the surface layer CH<sub>4</sub> Jacobians are plotted for the A-signal, D-signal and D/A ratio as a function of SZA.

610

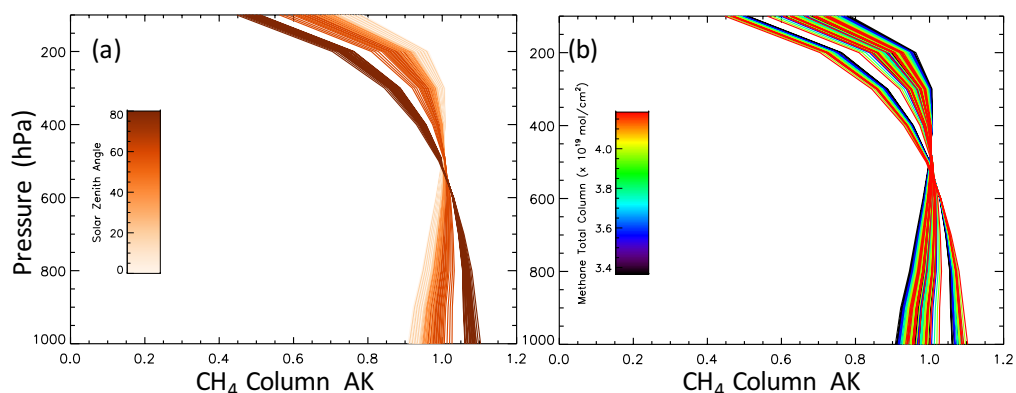


**Figure 16:** Variation of CHRONOS CH<sub>4</sub> averaging kernels for different SZA (left) and CH<sub>4</sub> total column (right) for 100 simulations with different SZA and CH<sub>4</sub> column values. Within each “group” of SZA values, the lesser AK dependence on low-to-high values of CH<sub>4</sub> can be seen.

615

## 6 Relationship of CHRONOS to Current and Future Missions

CHRONOS addresses key NASA science goals and National Research Council Decadal Survey questions, listed in Table 3, with heritage from past satellite instruments and opportunities for synergistic observations with current and upcoming LEO and GEO platforms. In particular, CHRONOS would complement planned NASA missions for air quality and carbon cycle science. It would deliver air pollutant measurements identified in the 2007 Decadal Survey GEO-CAPE mission (NRC, 2007) and address currently unmet science objectives described in the GEO-CAPE Science Traceability Matrix (Fishman et al., 2012).

### 6.1 Other Satellite CO Observations

Along with MOPITT, satellite measurements of CO in the MWIR (4.6  $\mu\text{m}$ ) are available from AIRS, a grating spectrometer on EOS-Aqua launched in 2002 (Aumman et al., 2003); the IASI FTS instruments on MetOp-A, B and C, launched in 2006, 2012 and expected in 2018 (Crevoisier et al., 2014); and the CrIS FTS instruments on Suomi NPP, launched 2011, and JPSS1-4 with projected launches starting in 2017 (Gambacorta et al., 2014). These LEO observations give daily global coverage at morning (IASI) and afternoon (AIRS, CrIS) equator crossings with sensitivity to CO in the middle troposphere for most observing conditions (George et al., 2009). The measurements are

630



expected to be available during the CHRONOS mission time frame, and will provide valuable intercomparisons for the MWIR CHRONOS CO channel.

TROPOMI, a UV-VIS-NIR-SWIR spectrometer, scheduled to launch in 2017, will provide daily  
635 global coverage from LEO at a 13:30 equator crossing with 7 km x 7 km spatial resolution and 10%  
column precision and 15% accuracy for SWIR (2.3  $\mu\text{m}$ ) CO observations (Veefkind et al., 2012).  
The TROPOMI CO measurements will provide true total column CO retrievals with more spatial  
coverage than MOPITT, but will not have MOPITT's CO vertical profile information. GOSAT-2  
(<http://www.gosat2.nies.go.jp>), with expected launch in 2017, will also measure SWIR CO bands but  
640 with measurements spaced around 200 km apart and large gaps in the ground sampling. CHRONOS  
multispectral CO measurements would provide vertical profiles of CO over the continental U.S.  
domain every 10 minutes, along with total column CO that can be compared to TROPOMI and  
GOSAT-2. The LEO observations of CO outside of the CHRONOS field of regard would be useful  
for constraining CO transported from sources outside North America.

## 645 **6.2 Other Satellite CH<sub>4</sub> Observations**

GOSAT, launched in 2009, measures CH<sub>4</sub> from LEO in the SWIR (1.6  $\mu\text{m}$ ), with relatively sparse  
coverage, a 10-km diameter footprint and column precision around 0.6% for single observations  
(Schepers et al., 2012). Improved sampling, coverage and precision are expected for GOSAT-2.  
Wecht et al. (2014a) show that hourly GEO SWIR CH<sub>4</sub> observations over California with 4 km x 4  
650 km spatial resolution and 1.1% precision provide about 20 times the information for estimating CH<sub>4</sub>  
emissions compared to 3 days of GOSAT observations. This means that 1 hour of CHRONOS data  
would provide more information than a year of GOSAT observations, assuming  $1/\sqrt{N}$  improvement  
for 365 days. Turner et al. (2015) used 3 years (2009-2011) of GOSAT CH<sub>4</sub> measurements to estimate  
North American emissions with  $1/2^\circ \times 2/3^\circ$  (~50 km x 70 km) spatial resolution, and found significant  
655 differences with the a priori inventory for anthropogenic emissions. Assuming the same information  
scaling found by Wecht et al. (2014a), CHRONOS would be able to quantify CH<sub>4</sub> emissions for this  
spatial scale on a daily basis, with the capability to assess more rapid emission changes for events  
such as the 2015 Aliso Canyon gas leak (Conley et al., 2016).

TROPOMI in LEO uses near infrared (NIR) 0.76  $\mu\text{m}$  and SWIR (2.3  $\mu\text{m}$ ) bands for CH<sub>4</sub>  
660 measurements and has an expected 0.6 % precision for single column CH<sub>4</sub> retrievals at 7 km x 7 km



spatial resolution (Butz et al., 2012). Based on an analysis in Jacob et al. (2016), TROPOMI should be capable of regional scale quantification of CH<sub>4</sub> emissions. The daily probability of viewing sources that are either transient or obscured by clouds would be higher for CHRONOS in GEO than for TROPOMI, since CHRONOS would observe the entire continental U.S. domain at least once during each daylight hour. CHRONOS also has a higher probability of cloud free observations given its smaller pixel size (see Figure 11).  
665

For emissions on a 1/2° x 2/3° grid, Wecht et al. (2014a) show that GEO-CAPE SWIR CH<sub>4</sub> hourly observations (assuming 1.1% column precision) have 2.4 times the information of daily TROPOMI for estimating CH<sub>4</sub> emissions. More work is needed using OSSEs to understand how to optimally exploit LEO observations of CH<sub>4</sub> and CO, especially from TROPOMI and GOSAT-2, in combination with the information on diurnal variability that CHRONOS could provide. This extends to examination of the North American carbon budget since CO and CH<sub>4</sub> measurements from CHRONOS, in conjunction with detailed CO<sub>2</sub> observations from planned and operating missions, would allow differentiation of anthropogenic combustion and wildfire sources of CO<sub>2</sub>.  
670

**Table 3.** Relevance of CHRONOS science objectives and measurements to NASA science goals, NRC questions and current and future missions

NASA Earth Science Goals	2014 NRC Questions	2007 CHRONOS Science Objectives	2007 CHRONOS Measurements	LEO Heritage	Synergy with Global Air Quality Constellation
Advance the understanding of changes in the Earth's radiation balance, air quality, and the ozone layer that result from changes in atmospheric composition	How will continuing economic development affect the production of air pollutants? How will [air] pollutants be transported across oceans and continents?	<b>O1. Quantify the temporal and spatial variations of CH<sub>4</sub> and CO emissions for air quality, climate, and energy decision making</b>	<b>CH<sub>4</sub> total column abundance: (O1)</b> Benefits: Unprecedented capability for quantifying North American emissions.	SCIAMACHY SWIR CH <sub>4</sub> (2002-2012) GOSAT SWIR CH <sub>4</sub> (2009-?)	<b>Correlative LEO measurements:</b> <ul style="list-style-type: none"> <li>EUMETSAT IASI and IASI-NG</li> <li>MMWR CO, O<sub>3</sub>, NH<sub>3</sub>, + other gases on METOP (2018-2035)</li> <li>NASA OCO-3 CO<sub>2</sub> on ISS (2017-?)</li> <li>ESA S5-P TROPOMI SWIR, UV-Vis CO, CH<sub>4</sub>, O<sub>3</sub>, + other gases (2017-2024)</li> <li>JAXA GOSAT-2</li> <li>SWIR CO<sub>2</sub>, CH<sub>4</sub>, CO, + other gases (2018-2023)</li> </ul>
Further the use of Earth system science research to inform decisions and provide benefit to society		<b>O2. Track rapidly changing vertical and horizontal atmospheric pollution transport to determine near-surface air quality at urban spatial scales, and at diurnal to monthly temporal scales</b>	<b>CO total column and tropospheric abundance in up to 3 layers with near-surface sensitivity: (O1 &amp; O2)</b> Benefits: Outstanding tracer of air pollution with temporal and spatial resolution to test predictions of air quality.	MAPS MMWR CO on Shuttle (1981-1994) MOPITT MMWR & SWIR (multispectral) CO (1999-2020(?)) SCIAMACHY SWIR CO (2002-2012) AIRS/TES/IASI/CrIS MMWR CO (2002-?)	<b>CHRONOS would provide CH<sub>4</sub> and multispectral CO measurements in the GEO constellation:</b> <ul style="list-style-type: none"> <li>Korean GEMS UV-Vis O<sub>3</sub>, aerosols + other gases on MP-GEOSAT (2018-2027)</li> <li>ESA/EUMETSAT Sentinel-4 UV-Vis O<sub>3</sub>, aerosols, + other gases</li> <li>MTG/MMWR O<sub>3</sub>, aerosols, CO, + other gases (2021-2028)</li> <li>NASA TEMPO UV-Vis O<sub>3</sub>, aerosols, + other gases; (2019-?)</li> </ul>







## 7 Conclusions

The CHRONOS investigation using 2-D imaging with full spectral resolution, would contribute the only sub-hourly CO and CH<sub>4</sub> observations for the U.S. component of an international GEO  
680 satellite constellation for atmospheric composition (CEOS, 2011) that includes the  
ESA/EUMETSAT Sentinel 4 mission over Europe and the Korean MP-GEOSAT/GEMS over  
Asia, along with the NASA TEMPO mission. LEO components (IASI, TROPOMI, GOSAT-2) of  
the constellation provide the global context (Table 3) for CHRONOS observations in assessing  
regional-to-global emissions and transport.

685 The main points defining the CHRONOS science investigation may be summarized as follows:

1. CHRONOS would deliver the first sub-hourly observation capability for comprehensive  
U.S. CH<sub>4</sub> and CO emission inventories and the ability to distinguish local from transported  
air pollution.
2. At the county scale, CHRONOS would enable new estimates of rapidly changing, highly  
690 variable CH<sub>4</sub> and CO emissions from growing natural gas extraction and increasingly  
frequent and severe wildfires. These emissions estimates are essential for air quality,  
climate, and energy management decisions.
3. The dense data from sub-hourly air pollution observations at fine spatial resolution  
(nominally 4 km × 4 km) over the entire greater North American domain would quantify  
695 diurnal changes in air pollution and discriminate different source regions for urban and  
rural emission activities.
4. CHRONOS' multispectral CO retrieval would provide vertical information near the  
surface in addition to the free troposphere to distinguish local air pollution from transported  
air pollution through horizontal and vertical tracking.
- 700 5. CHRONOS observations would strengthen the international air quality satellite  
constellation.

These science goals would be achieved by taking advantage of a simple, low-risk instrument  
design that is well suited to the CHRONOS CO and CH<sub>4</sub> measurements. The GCFR heritage  
follows the successful 17-year, on-orbit operation of MOPITT over a wide range of observing  
705 conditions. This technique provides for high effective spectral resolution for the target gases, high



signal levels compared to other types of spectrometers with similar spectral sensitivity, and small impact from signals due to interfering gases, aerosols, clouds and changing scene.

### Acknowledgements

710 This work was partly supported by NASA grant NNX15AK98G. The National Center for  
Atmospheric Research (NCAR) is sponsored by the National Science Foundation. The NCAR  
MOPITT project is supported by the NASA Earth Observing System Program. We thank Glenn  
Diskin and the DACOM measurement team at NASA Langley for providing the DISCOVER-AQ  
CH<sub>4</sub> measurements shown in Figure 3.

715

### References

- Abatzoglou, J. T. and Williams, A. P.: Impact of anthropogenic climate change on wildfire across  
western US forests, *Proceedings of the National Academy of Sciences*,  
DOI:10.1073/pnas.1607171113, 2016.
- 720 Acton, L. L., Griggs, M., Hall, G. D., Ludwig, C. B., Malkmus, W., Hesketh, W. D., and Reichle,  
H.: Remote measurement of carbon monoxide by a gas filter correlation instrument, *AIAA  
Journal*, 11(7), 899-900., 1973.
- Allen, D. T., Torres, V. M., et al.: Measurements of methane emissions at natural gas production  
sites in the United States, *Proceedings of the National Academy of Sciences*, 2013. Vol.  
725 110(44): p. 17768-17773. DOI: 10.1073/pnas.1304880110, 2013.
- Alvarez, R. A., Pacala, S. W., et al.: Greater focus needed on methane leakage from natural gas  
infrastructure, *Proceedings of the National Academy of Sciences*, Vol. 109 (17): p. 6435-6440,  
DOI:10.1073/pnas.1202407109, 2012.
- Anderson, G. P., Clough, S. A., Kneizys, F. X., Chetwynd, J. H. and Shettle, E. P., AFGL  
730 atmospheric constituent profiles (0–120 km), AFGL-TR-86-0110, AFGL(OPI), Air Force  
Geophysics Laboratory, Hanscom Air Force Base, MA 01736, USA, 1986.
- Anderson, D. C. et al., Measured and modeled CO and NO<sub>y</sub> in DISCOVER-AQ: An evaluation of  
emissions and chemistry over the eastern US, *Atmospheric Environment*, 96, 78–87,  
doi:10.1016/j.atmosenv.2014.07.004., 2014.



- 735 Angelbratt, J., Mellqvist, J., Blumenstock, T., Borsdorff, T., Brohede, S., Duchatelet, P.,  
Forster, F., Hase, F., Mahieu, E., Murtagh, D., Petersen, A. K., Schneider, M., Sussmann, R.,  
and Urban, J.: A new method to detect long term trends of methane (CH<sub>4</sub>) and nitrous oxide  
(N<sub>2</sub>O) total columns measured within the NDACC ground-based high resolution solar FTIR  
network, *Atmos. Chem. Phys.*, 11, 6167-6183, doi:10.5194/acp-11-6167-2011, 2011.
- 740 Arellano, A. F., Hess, P. G., et al.: Constraints on black carbon aerosol distribution from  
Measurement of Pollution in the Troposphere (MOPITT) CO, *Geophysical Research Letters*,  
2010. Vol. 37 (17): DOI:10.1029/2010gl044416, 2010.
- Aumann, H. H., Chahine, M. T., Gautier, C., Goldberg, M. D., Kalnay, E., McMillin, L., M.,  
Revercomb, H., Rosenkranz, P.W., Smith, W. L., Staelin, D. H., Strow, L. L., and Susskind,  
745 J.: AIRS/AMSU/HSB on the Aqua mission: Design, science objectives, data products, and  
processing systems, *IEEE T. Geosci. Remote Sens.*, 41, 2, 253–264, 2003.
- Barrie, L., Langen, A., J., Borrell, P., Boucher, O., Burrows, J., Camy-Peyret, C., Fishman, J., et  
al.: The changing atmosphere, An integrated global atmospheric chemistry observation theme  
for the IGOS partnership (IGACO). ESA SP 1282, 2004.
- 750 Bergamaschi, P., Frankenberg, C., et al.: Satellite cartography of atmospheric methane from  
SCIAMACHY on board ENVISAT: 2. Evaluation based on inverse model simulations, *Journal  
of Geophysical Research: Atmospheres*, Vol. 112 (D2), DOI: 10.1029/2006jd007268, 2007.
- Bergamaschi, P., Frankenberg, C., et al.: Inverse modeling of global and regional CH<sub>4</sub> emissions  
using SCIAMACHY satellite retrievals, *Journal of Geophysical Research: Atmospheres*, Vol.  
755 114(D22), DOI:10.1029/2009jd012287, 2009.
- Bian, H., Chin, M., et al.: Multiscale carbon monoxide and aerosol correlations from satellite  
measurements and the GOCART model: Implication for emissions and atmospheric  
atmospheric evolution, *Journal of Geophysical Research: Atmospheres*, Vol. 115 (D7),  
DOI:10.1029/2009jd012781, 2010.
- 760 Bloom, A. A., Worden, J., Jiang, Z., Worden, H., Kurosu, T., Frankenberg, C., and Schimel, D.:  
Remote-sensing constraints on South America fire traits by Bayesian fusion of atmospheric  
and surface data, *Geophys. Res. Lett.*, 42 (4), doi:10.1002/2014GL062584, 2015.
- Bohren, C. F., and Huffman, D. R.: *Absorption and Scattering of Light by Small Particles*, John  
Wiley, New York, 1983.



- 765 Bousserez, N., Henze, D. K., Rooney, B., Perkins, A., Wecht, K. J., Turner, A. J., Natraj, V., and  
Worden, J. R.: Constraints on methane emissions in North America from future geostationary  
remote-sensing measurements, *Atmos. Chem. Phys.*, 16, 6175-6190, doi:10.5194/acp-16-  
6175-2016, 2016.
- Breul, H., et al.: U.S. Expected to be Largest Producer of Petroleum and Natural Gas Hydrocarbons  
770 in 2013. *Today in Energy*, <http://www.eia.gov/todayinenergy/detail.cfm?id=13251>, 2013.
- Brunekreef, B., and Holgate, S. T.: Air pollution and health, *The Lancet*. Vol. 360 (9341): p. 1233-  
1242. DOI: 10.1016/s0140-6736(02)11274-8, 2002.
- Butz, A., Galli, A., Hasekamp, O., Landgraf, J., Tol, P., and Aben, I.: TROPOMI aboard Precursor  
Sentinel-5 Precursor: Prospective performance of CH<sub>4</sub> retrievals for aerosol and cirrus loaded  
775 atmospheres, *Remote Sens. Environ.*, 120, 267–276, doi:10.1016/j.rse.2011.05.030, 2012.
- Ciais, P., Sabine, C., Bala, G., Bopp, L., Brovkin, V., Canadell, J., Chhabra, A., DeFries, R.,  
Galloway, J., Heimann, M., Jones, C., Le Quéré, C., Myneni, R. B., Piao S., and Thornton P.;  
Carbon and Other Biogeochemical Cycles. In: *Climate Change 2013: The Physical Science  
Basis. Contribution of Working Group I to the Fifth Assessment Report of the  
780 Intergovernmental Panel on Climate Change* [Stocker, T. F., Qin, D., Plattner, M.,  
Tignor, S. K. Allen, J., Boschung, A., Nauels, Y., Xia, V. Bex and P. M. Midgley (eds.)].  
Cambridge University Press, Cambridge, United Kingdom and New York, NY, USA, pp. 465  
– 570, doi:10.1017/CBO9781107415324.015, 2013.
- CEOS: A Geostationary Satellite Constellation for Observing Global Air Quality: An International  
785 Path Forward,  
[http://www.ceos.org/index.php?option=com\\_content&view=category&layout=blog&id=54&  
Itemid=95](http://www.ceos.org/index.php?option=com_content&view=category&layout=blog&id=54&Itemid=95), 2011.
- Clerbaux, C., Boynard, A., Clarisse, L., George, M., Hadji-Lazaro, J., Herbin, H., Hurtmans, D.,  
Pommier, M., Razavi, A., Turquety, S., Wespes, C., and Coheur, P.-F.: Monitoring of  
790 atmospheric composition using the thermal infrared IASI/MetOp sounder, *Atmos. Chem.  
Phys.*, 9, 6041-6045, 2009.
- Conley, S., et al.: Methane emissions from the 2015 Aliso Canyon blowout in Los Angeles, CA.  
*Science*, DOI: 10.1126/science.aaf.2348, 2016.
- Crevoisier, C., Clerbaux, C., Guidard, V., Phulpin, T., Armante, R., Barret, B., Camy-Peyret, C.,  
795 Chaboureaud, J.-P., Coheur, P.-F., Crépeau, L., Dufour, G., Labonnote, L., Lavanant, L., Hadji-



- Lazaro, J., Herbin, H., Jacquinet-Husson, N., Payan, S., Péquignot, E., Pierangelo, C., Sellitto, P., and Stubenrauch, C.: Towards IASI-New Generation (IASI-NG): impact of improved spectral resolution and radiometric noise on the retrieval of thermodynamic, chemistry and climate variables, *Atmos. Meas. Tech.*, 7, 4367-4385, doi:10.5194/amt-7-4367-2014, 2014.
- 800 Deeter, M. N., Emmons, L. K., Edwards, D. P., Gille, J. C., and Drummond, J. R.: Vertical resolution and information content of CO profiles retrieved by MOPITT, *Geophysical Research Letters*, 31, 15112, doi:10.1029/2004GL020235, 2004.
- Deeter, M. N., Edwards, D. P., Gille, J. C., and Drummond, J. R.: CO retrievals based on MOPITT near-infrared observations, *Journal of Geophysical Research (Atmospheres)*, 114(d13), 4303, 805 doi:10.1029/2008JD010872, 2009.
- Deeter, M. N., Worden, H. M., Gille, J. C., Edwards, D. P., Mao, D., and Drummond, J. R.: MOPITT multispectral CO retrievals: Origins and effects of geophysical radiance errors, *Journal of Geophysical Research: Atmospheres*, 116 (D15), doi:10.1029/2011JD015703, 2011.
- 810 Deeter, M. N., Martínez-Alonso, S., Edwards, D. P., Emmons, L. K., Gille, J. C., Worden, H. M., Pittman, J. V., Daube, B. C., and Wofsy, S. C.: Validation of MOPITT Version 5 thermal-infrared, near-infrared, and multispectral carbon monoxide profile retrievals for 2000–2011, *Journal of Geophysical Research: Atmospheres*, doi:10.1002/jgrd.50272, 2013.
- Drummond, J.R., J. Zou, F. Nichitiu, J. Kar, R. Deschambaut, J. Hackett: A review of 9-year 815 performance and operation of the MOPITT instrument, *J. Adv. Space Res.*, doi:10.1016/j.asr.2009.11.019, 2010.
- Edwards, D. P., Halvorson, C. M., and Gille, J. C.: Radiative transfer modeling for the EOS Terra satellite Measurement of Pollution in the Troposphere (MOPITT) instrument, *Journal of Geophysical Research: Atmospheres*, 104(D14), 16755–16775, doi:10.1029/1999JD900167, 820 1999.
- Edwards, D. P.; Emmons, L. K.; et al.: Observations of carbon monoxide and aerosols from the Terra satellite: Northern Hemisphere variability. *Journal of Geophysical Research: Atmospheres*, Vol. 109(D24), DOI:10.1029/2004jd004727, 2004.
- Edwards, D. P., Arellano, A. F., and Deeter, M. N.: A satellite observation system simulation 825 experiment for carbon monoxide in the lowermost troposphere, *J. Geophys. Res.-Atmos.*, 114, doi:10.1029/2008JD011375, 2009.



- Emmons, L. K., Edwards, D. P., Deeter, M. N., Gille, J. C., Campos, T., Nédélec, P., Novelli, P.,  
and Sachse, G.: Measurements of Pollution In The Troposphere (MOPITT) validation through  
2006, *Atmos. Chem. Phys.*, 9, 1795-1803, doi  
830 ., 2011.
- Fann, N., Lamson, A. D., et al.: Estimating the National Public Health Burden Associated with  
Exposure to Ambient PM<sub>2.5</sub> and Ozone, *Risk Analysis*, Vol. 32(1): p. 81-95. DOI:  
10.1111/j.1539-6924.2011.01630.x, 2012.
- Fisher, J. A., Jacob, D. J., et al.: Source attribution and interannual variability of Arctic pollution  
835 in spring constrained by aircraft (ARCTAS, ARCPAC) and satellite (AIRS) observations of  
carbon monoxide, *Atmos. Chem. Phys.*, Vol. 10(3): p. 977-996. DOI: 10.5194/acp-10-977-  
2010, 2010.
- Fishman, J., Iraci, L. T., et al.: The United States' Next Generation of Atmospheric Composition  
and Coastal Ecosystem Measurements: NASA's Geostationary Coastal and Air Pollution  
840 Events (GEO-CAPE) Mission, *Bulletin of the American Meteorological Society*, 2012. Vol.  
93(10): p. 1547-1566. DOI: 10.1175/bams-d-11-00201.1, 2012.
- Flynn, L., et al.: Performance of the Ozone Mapping and Profiler Suite (OMPS) products, *J.  
Geophys. Res. Atmos.*, 119, 6181–6195, doi:10.1002/2013JD020467, 2014.
- Fortems-Cheiney, A., Chevallier, F., Pison, I., Bousquet, P., Szopa, S., Deeter, M. N., and  
845 Clerbaux, C.: Ten years of CO emissions as seen from Measurements of Pollution in the  
Troposphere (MOPITT), *J. Geophys. Res.*, 116, D05304, doi:10.1029/2010JD014416., 2011.
- Frankenberg, C., Meirink, J. F., van Weele, M., Platt, U., and Wagner, T.: Assessing Methane  
Emissions from Global Space-Borne Observations, *Science*, Vol. 308 (5724), p. 1010-1014,  
doi:10.1126/science.1106644, 2005.
- 850 Frankenberg, C., Aben, I., Bergamaschi, P., Dlugokencky, E. J., van Hees, R., Houweling, S., van  
der Meer, P., Snel, R., and Tol, P.: Global column averaged methane mixing ratios from 2003  
to 2009 as derived from SCIAMACHY: Trends and variability, *J. Geophys. Res.*, 116,  
D04302, doi:10.1029/2010JD014849, 2011.
- GACS: Global Monitoring for Environment and Security Atmosphere Core Service (GACS), in  
855 Implementation Group – Final Report, 2009.
- Galmarini, S., Koffi, B., Solazzo, E., Keating, T., Hogrefe, C., Schulz, M., Benedictow, A.,  
Griesfeller, J.J., Janssens-Maenhout, G., Carmichael, G. and Fu, J.: Technical note:



- 860 Coordination and harmonization of the multi-scale, multi-model activities HTAP2, AQMEII3, and MICS-Asia3: simulations, emission inventories, boundary conditions, and model output formats. *Atmospheric Chemistry and Physics*, 17(2), pp.1543-1555, 2017.
- Gambacorta, A., Barnet, C., Wolf, W., King, T., Maddy, E., Strow, L., Xiong, X., Nalli, N., and Goldberg, M.: An Experiment Using High Spectral Resolution CrIS Measurements for Atmospheric Trace Gases: Carbon Monoxide Retrieval Impact Study, *IEEE Geosci. Remote S.*, 11, 1639–1643, 2014.
- 865 Garnett, J. D., Farris, M. C., Wong, S. S., Zandian, M., Hall, D. N., Jacobson, S., Luppino, G., et al.: 2Kx2K molecular beam epitaxy HgCdTe detectors for the James Webb Space Telescope NIRCam instrument. In *SPIE Astronomical Telescopes+ Instrumentation*, pp. 35–46. International Society for Optics and Photonics, 2004.
- Gaubert, B., et al.: Toward a chemical reanalysis in a coupled chemistry-climate model: An evaluation of MOPITT CO assimilation and its impact on tropospheric composition, *J. Geophys. Res. Atmos.*, 121, 7310–7343, doi:10.1002/2016JD024863, 2016.
- 870 George, M., Clerbaux, C., Hurtmans, D., Turquety, S., Coheur, P.-F., Pommier, M., Hadji-Lazaro, J., Edwards, D. P., Worden, H., Luo, M., Rinsland, C., and McMillan, W.: Carbon monoxide distributions from the IASI/METOP mission: evaluation with other spaceborne remote sensors, *Atmos. Chem. Phys.*, 9:8317-8330, 2009.
- 875 Gloudemans, A. M. S., Schrijver, H., Hasekamp, O. P., and Aben, I.: Error analysis for CO and CH<sub>4</sub> total column retrievals from SCIAMACHY 2.3μm spectra, *Atmos. Chem. Phys.*, 8, 3999-4017, 2008.
- Green, R. O., et al.: The Moon Mineralogy Mapper (M<sup>3</sup>) imaging spectrometer for lunar science: Instrument description, calibration, on-orbit measurements, science data calibration and on-orbit validation, *J. Geophys. Res.*, 116, E00G19, doi:10.1029/2011JE003797, 2011.
- 880 Grell, G., Peckham, S., Schmitz, R., McKeen, S., Frost, G., Skamarock, W., and Eder, B.: Fully coupled “online” chemistry within the WRF model, *Atmos. Environ.*, 39(37), 6957–6975, doi:10.1016/j.atmosenv.2005.04.027, 2005.
- 885 Guizar-Sicairos, M., Thurman, S. T., et al.: Efficient subpixel image registration algorithms, *Optics Letters*, Vol. 33(2): p. 156-158, DOI:10.1364/ol.33.000156, 2008.





- He, H. et al.: Trends in emissions and concentrations of air pollutants in the lower troposphere in the Baltimore/Washington airshed from 1997 to 2011, *Atmos. Chem. Phys.*, 13(15), 7859–7874, doi:10.5194/acp-13-7859-2013, 2013.
- 890 Heidinger, A.: ABI Cloud Mask Algorithm Theoretical Basis Document, NOAA, 2011. [http://www.goes-r.gov/products/ATBDs/baseline/Cloud\\_CldMask\\_v2.0\\_no\\_color.pdf](http://www.goes-r.gov/products/ATBDs/baseline/Cloud_CldMask_v2.0_no_color.pdf) (last accessed 6 Oct. 2016)
- Hess, M., Koepke, P., and Schult, I.: Optical properties of aerosols and clouds: The software package OPAC, *Bull. Amer. Meteorol. Soc.*, 79(5), 831–844, 1998.
- 895 Holloway, T., H. Levy II, and P. Kasibhatla: Global distribution of carbon monoxide, *J. Geophys. Res.*, 105(D10), 12,123–12,147, 2000.
- Howard, T., Ferrara, T. W., et al.: Sensor transition failure in the high flow sampler: Implications for methane emission inventories of natural gas infrastructure, *Journal of the Air & Waste Management Association*, DOI:10.1080/10962247.2015.1025925, 2015.
- 900 Huang, M., Bowman, K. W., Carmichael, G. R., Pierce, R. B., Worden, H. M., Luo, M., Cooper, O. R., Pollack, I. B., Ryerson, T. B., and Brown, S. S.: Impact of Southern California anthropogenic emissions on ozone pollution in the mountain states: Model analysis and observational evidence from space, *J. Geophys. Res. Atmos.*, 118, doi:10.1002/2013JD020205, 2013.
- 905 Hudman, R. C., Murray, L. T., et al.: "Biogenic versus anthropogenic sources of CO in the United States." *Geophysical Research Letters*, Vol. 35(4), DOI:10.1029/2007gl032393, 2008.
- Jacob, D. J., Turner, A. J., et al.: Satellite observations of atmospheric methane and their value for quantifying methane emissions." *Atmos. Chem. Phys.*, DOI: 10.5194/acp-2016-555, 2016.
- Jiang, Z., Jones, D. B. A., Worden, J., Worden, H. M., Henze, D. K., and Wang, Y. X.: Regional data assimilation of multi-spectral MOPITT observations of CO over North America, *Atmos. Chem. Phys.*, 15(12), 6801–6814, doi:10.5194/acp-15-6801-2015, 2015.
- 910 Jiang, Z., Jones, D. B. A., Worden, H. M., Deeter, M. N., Henze, D. K., Worden, J., Bowman, K. W., Brenninkmeijer, C. a. M., and Schuck, T. J.: Impact of model errors in convective transport on CO source estimates inferred from MOPITT CO retrievals, *Journal of Geophysical Research: Atmospheres*, 118(4), 2073–2083, doi:10.1002/jgrd.50216, 2013.
- 915



- Karion, A., Sweeney, C., et al.: Methane emissions estimate from airborne measurements over a western United States natural gas field, *Geophysical Research Letters*, Vol. 40(16): p. 4393-4397. DOI:10.1002/grl.50811, 2013.
- 920 Katzenstein, A. S., Doezema, L. A., et al.: Extensive regional atmospheric hydrocarbon pollution in the southwestern United States, *Proceedings of the National Academy of Sciences*, Vol. 100(21): p. 11975-11979. DOI:10.1073/pnas.1635258100, 2003.
- Kopacz, M., Jacob, D. J., et al.: Comparison of adjoint and analytical Bayesian inversion methods for constraining Asian sources of carbon monoxide using satellite (MOPITT) measurements of CO columns, *Journal of Geophysical Research: Atmospheres*, Vol. 114(D04305): p. 1-10.,  
925 2009.
- Kopacz, M., Jacob, D. J., et al.: Global estimates of CO sources with high resolution by adjoint inversion of multiple satellite datasets (MOPITT, AIRS, SCIAMACHY, TES), *Atmos. Chem. Phys.*, Vol. 10(3): p. 855-876. DOI: 10.5194/acp-10-855-2010, 2010.
- Kort, E. A., Eluszkiewicz, J., et al.: Emissions of CH<sub>4</sub> and N<sub>2</sub>O over the United States and Canada  
930 based on a receptor-oriented modeling framework and COBRA-NA atmospheric observations, *Geophysical Research Letters*, Vol. 35(18), DOI: 10.1029/2008gl034031, 2008.
- Lee, S., Hong, Y., et al.: Plan of Korean Geostationary Environment Satellite over Asia- Pacific region. in EGU General Assembly 2010. Vienna, Austria, 2010.
- Levi, A, Simonds, J., and Gruber, C.: CHIRP Technology Demonstration Project. In AIAA  
935 SPACE 2011 Conference & Exposition, p. 7333, 2011
- P. F. Levelt et al.: The ozone monitoring instrument, *IEEE Transactions on Geoscience and Remote Sensing*, vol. 44, no. 5, pp. 1093-1101, doi: 10.1109/TGRS.2006.872333, 2006.
- Loomis, D., Grosse, Y., et al.: The carcinogenicity of outdoor air pollution, *The Lancet Oncology*. Vol. 14(13): p. 1262-1263. DOI: 10.1016/s1470-2045(13)70487-X, 2013
- 940 Ludwig, C. B., Malkmus, W., Griggs, M., & Bartle, E. R.: Monitoring of Air Pollution by Satellites (MAPS), phase 1, NASA-CR-2324, 1972.
- Malley, C. S., Kuylenstierna, J. C., Vallack, H. W., Henze, D. K., Blencowe, H., and Ashmore, M. R.: Preterm birth associated with maternal fine particulate matter exposure: A global, regional and national assessment. *Environment international*,  
945 <https://doi.org/10.1016/j.envint.2017.01.023>, 2017.



- Massie, S. T., Gille, J. C., Edwards, D. P., and Nandi, S.: Satellite observations of aerosol and CO  
over Mexico City, *Atmospheric Environment*, 40(31), 6019–6031,  
doi:10.1016/j.atmosenv.2005.11.065, 2006.
- Meirink, J. F., Bergamaschi, P., et al.: Four-dimensional variational data assimilation for inverse  
950 modeling of atmospheric methane emissions: Analysis of SCIAMACHY observations, *Journal  
of Geophysical Research: Atmospheres*, Vol. 113(D17), DOI: 10.1029/2007jd009740, 2008.
- Miller, S. M., Matross, D. M., et al.: Sources of carbon monoxide and formaldehyde in North  
America determined from high-resolution atmospheric data, *Atmos. Chem. Phys.*, Vol. 8(24):  
p. 7673-7696. DOI: 10.5194/acp-8-7673-2008, 2008.
- 955 Miller, S. M., Wofsy, S. C., Michalak, A. M., Kort, E. A., Andrews, A. E., Biraud, S. C.,  
Dlugokencky, E. J., Eluszkiewicz, J., Fischer, M. L., Janssens-Maenhout, G., Miller, B. R.,  
Miller, J. B., Montzka, S. A., Nehrkorn, T., and Sweeney, C.: Anthropogenic emissions of  
methane in the United States, *Proc. Natl. Acad. Sci.*, 110, 50, 20018-20022,  
[www.pnas.org/cgi/doi/10.1073/pnas.1314392110](http://www.pnas.org/cgi/doi/10.1073/pnas.1314392110), 2013.
- 960 Morino, I., et al.: Preliminary validation of column-averaged volume mixing ratios of carbon  
dioxide and methane retrieved from GOSAT short-wavelength infrared spectra, *Atmos. Meas.  
Tech.*, 4, 1061-1076, doi:10.5194/amt-4-1061-2011., 2011.
- Myhre, G., et al.: Anthropogenic and Natural Radiative Forcing. The Physical Science Basis.  
Contribution of Working Group I to the Fifth Assessment Report of the Intergovernmental  
965 Panel on Climate Change 2013, Cambridge, United Kingdom and New York, NY, USA:  
Cambridge University Press [http://www.ipcc.ch/pdf/assessment-  
report/ar5/wg1/WG1AR5\\_Chapter08\\_FINAL.pdf](http://www.ipcc.ch/pdf/assessment-report/ar5/wg1/WG1AR5_Chapter08_FINAL.pdf), 2013.
- Nédélec P., Blot R., Boulanger D., Athier, G., Cousin, J-M., Gautron, B., Petzold, A., Volz-  
Thomas, A. and Thouret, V.: Instrumentation on commercial aircraft for monitoring the  
970 atmospheric composition on a global scale: the IAGOS system, technical overview of ozone  
and carbon monoxide measurements, MOZAIC-IAGOS special issue, *Tellus B*, 67, 27791,  
<http://dx.doi.org/10.3402./tellusb.v67.27791>, 2015.
- Neil, D. O., Gordley, L. L., Marshall, B. T., and Sachse, G. W.: Tropospheric carbon monoxide  
measurements from geostationary orbit. In *Europto Remote Sensing* (pp. 265-273).  
975 International Society for Optics and Photonics, 2001.



- (NRA), N. R. C.: Earth Science and Applications from Space: National Imperatives for the Next Decade and Beyond, Washington, DC: The National Academies Press. 456, 2007.
- National Research Council: Air Quality Management in the United States. Washington, DC: The National Academies Press. doi:<https://doi.org/10.17226/10728>, 2004.
- 980 Palmer, P. I., Suntharalingam, P., et al.: Using CO<sub>2</sub>:CO correlations to improve inverse analyses of carbon fluxes, *Journal of Geophysical Research: Atmospheres*, Vol. 111(D12), DOI:10.1029/2005jd006697, 2006.
- Payne, V. H., Clough, S. A., Shephard, M. W., Nassar, R., and Logan, J. A.: Information-centered representation of retrievals with limited degrees of freedom for signal: Application to methane
- 985 from the Tropospheric Emission Spectrometer, *J. Geophys. Res.*, doi:10.1029/2008JD010155, 2009.
- Pechony, O., Shindell, D. T., et al.: Direct top-down estimates of biomass burning CO emissions using TES and MOPITT versus bottom-up GFED inventory, *Journal of Geophysical Research: Atmospheres*, Vol. 118(14): p. 8054-8066. DOI:10.1002/jgrd.50624, 2013.
- 990 Pétron, G., Frost, G., et al.: Hydrocarbon emissions characterization in the Colorado Front Range: A pilot study, *Journal of Geophysical Research: Atmospheres*, Vol. 117(D4): p. D04304, DOI:10.1029/2011jd016360, 2012.
- Pfister, G., Gille, J. C., Ziskin, D., Francis, G., Edwards, D. P., Deeter, M. N., and Abbott, E.: Effects of a Spectral Surface Reflectance on Measurements of Backscattered Solar Radiation:
- 995 Application to the MOPITT Methane Retrieval, *J. Atmos. Oceanic Technol.*, 22, 566, doi:10.1175/JTECH1721.1\_2005.
- Pfister, G. G., Reddy, P., Barth, M. C., Flocke, F. F., Fried, A., Herndon, S. C., Sive, B. C., Sullivan, J. T., Thompson, A. M., Yacovitch, T. I., Weinheimer, A. J., Wisthaler, A.: Using observations and source specific model tracers to characterize pollutant transport during
- 1000 FRAPPÉ and DISCOVER-AQ, submitted to *J. Geophys. Res.*, 2017.
- Pickett-Heaps, C. A., Jacob, D. J., Wecht, K. J., Kort, E. A., Wofsy, S. C., Diskin, G. S., Worthy, D. E. J., Kaplan, J. O., Bey, I., and Drevet, J.: Magnitude and seasonality of wetland methane emissions from the Hudson Bay Lowlands (Canada), *Atmos. Chem. Phys.*, 11, 3773-3779, doi:10.5194/acp-11-3773-2011, 2011.



- 1005 Reichle H.G. Jr., et al.: Space shuttle based global CO measurements during April and October 1994, MAPS instrument, data reduction, and data validation, *J. Geophys. Res.*, vol. 104, no. D17 pp 21443-21454, 1999.
- Rodgers, C. D., Wells, R. J., Grainger, R. G., Taylor, F. W.: Improved stratospheric and mesospheric sounder validation: General approach and in-flight radiometric calibration, *J. Geophys. Res.*, 101, 9775–9793, 1996.
- 1010 Rodgers, C. D.: *Inverse Methods for Atmospheric Sounding - Theory and Practice*. Series on Atmospheric Oceanic and Planetary Physics, Vol. 2. World Scientific Publishing Co. Pte. Ltd., 2000.
- Russell, J. M. III, Gordley, L. L., Park, J. H., Drayson, S. R., Hesketh, D. H., Cicerone, R. J., Tuck, A. F., Frederick, J. E., Harries, J. E., and Crutzen, P.: The Halogen Occultation Experiment, *J. Geophys. Res.*, Vol. 98, No. D6, 10,777-10,797, 1993.
- 1015 Russell, P. B., et al.: Aerosol-induced radiative flux changes off the United States mid-Atlantic coast: Comparison of values calculated from sunphotometer and in situ data with those measured by airborne pyranometer. *J. Geophys. Res.*, 104, 2289–2307, 1999.
- 1020 Schepers, D., Guerlet, S., Butz, A., Landgraf, J., Frankenberg, C., Hasekamp, O., Blavier, J.-F., Deutscher, N. M., Griffith, D. W. T., Hase, F., Kyro, E., Morino, I., Sherlock, V., Sussmann, R., and Aben, I.: Methane retrievals from Greenhouse Gases Observing Satellite (GOSAT) shortwave infrared measurements: Performance comparison of proxy and physics retrieval algorithms, *J. Geophys. Res.*, 117, D10307, doi:10.1029/2012JD017549, 2012.
- 1025 Schneising, O., Burrows, J. P., et al.: Remote sensing of fugitive methane emissions from oil and gas production in North American tight geologic formations, *Earth's Future*, Vol. 2(10): p. 548-558. DOI:10.1002/2014ef000265, 2014.
- Schwietzke, S., Sherwood, O. A., et al.: Upward revision of global fossil fuel methane emissions based on isotope database." *Nature*, Vol. 538(7623): p. 88-91. DOI:10.1038/nature19797, 2016.
- 1030 Silva, S. J., Arellano, A. F., and Worden, H. M.: Toward anthropogenic combustion emission constraints from space-based analysis of urban CO<sub>2</sub>/CO sensitivity. *Geophysical Research Letters*, Vol. 40 (18), p. 4971-4976, DOI:10.1002/grl.50954, 2013.
- Shindell, D. T., Faluvegi, G., et al.: "Improved Attribution of Climate Forcing to Emissions." *Science*, Vol. 326(5953): p. 716-718. DOI:10.1126/science.1174760, 2009.
- 1035



- Simmons, A., Fellous, J.-L., et al.: "Observation and integrated Earth-system science: A roadmap for 2016–2025." *Advances in Space Research*, Vol. 57(10): p. 2037-2103, DOI:10.1016/j.asr.2016.03.008, 2016.
- 1040 Spurr, R. J. D.: VLIDORT: A linearized pseudo-spherical vector discrete ordinate radiative transfer code for forward model and retrieval studies in multilayer multiple scattering media, *J Quant Spectrosc Radiat Transfer*, 102, 316-343, doi:10.1016/j.jqsrt.2006.05.005\_2006.
- Tolton, B. T., and Drummond, J. R.: Characterization of the length-modulated radiometer, *Applied Optics*, Vol. 36 (22), p. 5409-5420, <http://ao.osa.org/abstract.cfm?URI=ao-36-22-5409>, 10.1364/ao.36.005409, 1997.
- 1045 Trasande, L., Malecha, P., and Attina, T. M.: Particulate matter exposure and preterm birth: estimates of US attributable burden and economic costs. *Environmental health perspectives*, 124(12), 1913, <http://dx.doi.org/10.1289/ehp.1510810>, 2016.
- 1050 Turner, A. J., Jacob, D. J., Wecht, K. J., Maasakkers, J. D., Lundgren, E., Andrews, A. E., Biraud, S. C., Boesch, H., Bowman, K. W., Deutscher, N. M., Dubey, M. K., Griffith, D. W. T., Hase, F., Kuze, A., Notholt, J., Ohyama, H., Parker, R., Payne, V. H., Sussmann, R., Sweeney, C., Velazco, V. A., Warneke, T., Wennberg, P. O., and Wunch, D.: Estimating global and North American methane emissions with high spatial resolution using GOSAT satellite data, *Atmos. Chem. Phys.*, 15, 7049-7069, doi:10.5194/acp-15-7049-2015, 2015.
- 1055 Turner, A. J., Jacob, D. J., Benmergui, J., Wofsy, S. C., Maasakkers, J. D., Butz, A., Hasekamp, O., and Biraud, S. C.: A large increase in U.S. methane emissions over the past decade inferred from satellite data and surface observations, *Geophys. Res. Lett.*, 43, 2218–2224, doi:10.1002/2016GL067987, 2016.
- 1060 Turner, M. C., Jerrett, M., et al.: Long-Term Ozone Exposure and Mortality in a Large Prospective Study, *American Journal of Respiratory and Critical Care Medicine*, Vol. 193(10): p. 1134-1142. DOI: 10.1164/rccm.2015081633OC, 2015.
- UNEP: Near-term Climate Protection and Clean Air Benefits: Actions for Controlling Short-Lived Climate Forcers. Nairobi, Kenya: United Nations Environment Programme (UNEP). 78. <http://www.unep.org/publications/ebooks/SLCF/>, 2011.



- 1065 U.S.: Air Quality Criteria for Carbon Monoxide, U.S. Department of Health, Education, and  
Welfare, Public Health Service, National Air Pollution Control Administration Publication No.  
AP-62, March 19, 1970.
- Veefkind, J.P., Aben, I., McMullan, K., Forster, H., de Vries, J., Otter, G., Claas, J., Eskes, H.J.,  
de Haan, J.F., Kleipool, Q., van Weele, M., Hasekamp, O., Hoogeveen, R., Landgraf, J., Snel,  
1070 R., Tol, P., Ingmann, P., Voors, R., Kruizinga, B., Vink, R., Visser, H., and Levelt, P.F.:  
TROPOMI on the ESA Sentinel-5 Precursor: A GMES mission for global observations of the  
atmospheric composition for climate, air quality and ozone layer applications, *Remote Sensing  
of Environment* 120, 70-83, doi:10.1016/j.rse.2011.09.027, 2012.
- Vijayaraghavan, K., Snell, H. E., et al.: Practical Aspects of Using Satellite Data in Air Quality  
1075 Modeling, *Environmental Science & Technology*, Vol. 42(22): p. 8187-8192,  
DOI:10.1021/es7031339, 2008.
- Warner, J. X., Gille, J. C., Edwards, D. P., Ziskin, D. C., Smith, M. W., Bailey, P. L., and Rokke,  
L.: Cloud Detection and Clearing for the Earth Observing System Terra Satellite  
Measurements of Pollution in the Troposphere (MOPITT) Experiment, *Appl. Opt.*, 40(8),  
1080 1269–1284, doi:10.1364/AO.40.001269, 2001.
- Wecht, K. J., Jacob, D. J., Sulprizio, M. P., Santoni, G. W., Wofsy, S. C., Parker, R., Bösch, H.,  
and Worden, J.: Spatially resolving methane emissions in California: constraints from the  
CalNex aircraft campaign and from present (GOSAT, TES) and future (TROPOMI,  
geostationary) satellite observations, *Atmos. Chem. Phys.*, 14, 8173-8184, doi:10.5194/acp-  
1085 14-8173-2014, 2014(a).
- Wecht, K. J., Jacob, D. J., Frankenberg, C., Jiang, Z., and Blake, D. R.: Mapping of North  
American methane emissions with high spatial resolution by inversion of SCIAMACHY  
satellite data, *J. Geophys. Res. Atmos.*, 119, 7741–7756, doi:10.1002/2014JD021551, 2014(b).
- West, J. J., Fiore, A. M., et al.: Global health benefits of mitigating ozone pollution with methane  
1090 emission controls, *Proceedings of the National Academy of Sciences of the United States of  
America*, Vol. 103(11): p. 3988-3993, DOI:10.1073/pnas.0600201103, 2006.
- Westerling, A. L., Hidalgo, H. G., et al.: "Warming and Earlier Spring Increase Western U.S.  
Forest Wildfire Activity." *Science*, Vol. 313(5789): p. 940-943.  
DOI:10.1126/science.1128834, 2006.





- 1095 Worden, H. M., Deeter, M. N., Edwards, D. P., Gille, J. C., Drummond, J. R., and P. Nédélec:  
Observations of near-surface carbon monoxide from space using MOPITT multispectral  
retrievals, *Journal of Geophysical Research (Atmospheres)*, 115(d14), 18314,  
doi:10.1029/2010JD014242, 2010.
- Worden, H. M., Cheng, Y., Pfister, G., Carmichael, G. R., Zhang, Q., Streets, D. G., Deeter, M.,  
1100 Edwards, D. P., Gille, J. C., and Worden, J. R.: Satellite-based estimates of reduced CO and  
CO<sub>2</sub> emissions due to traffic restrictions during the 2008 Beijing Olympics, *Geophys. Res.  
Lett.*, 39, L14802, doi:10.1029/2012GL052395, 2012.
- Worden, H.M., et al.: Decadal Record of Satellite Carbon Monoxide Observations, *Atmos. Chem.  
Phys.*, doi:10.5194/acp-13-837-2013, 2013.
- 1105 Worden, J., Wecht, K., Frankenberg, C., Alvarado, M., Bowman, K., Kort, E., Kulawik, S., Lee,  
M., Payne, V., and Worden, H.: CH<sub>4</sub> and CO distributions over tropical fires during October  
2006 as observed by the Aura TES satellite instrument and modeled by GEOS-Chem, *Atmos.  
Chem. Phys.*, 13(7), 3679–3692, doi:10.5194/acp-13-3679-2013, 2013.
- Worden, J., Jiang, Z., et al.: "El Niño, the 2006 Indonesian peat fires, and the distribution of  
1110 atmospheric methane." *Geophysical Research Letters*, Vol. 40(18): p. 4938-4943. DOI:  
10.1002/grl.50937, <http://dx.doi.org/10.1002/grl.50937>, 2013.
- Wunch, D., et al.: Calibration of the Total Carbon Column Observing Network using aircraft  
profile data, *Atmos. Meas. Tech.*, 3, 1351-1362, doi:10.5194/amt-3-1351-2010, 2010.
- Xiao, Y., Logan, J. A., et al.: Global budget of ethane and regional constraints on U.S. sources,  
1115 *Journal of Geophysical Research: Atmospheres*, Vol. 113(D21), DOI: 10.1029/2007jd009415,  
2008.
- Zhang, L., Jacob, D. J., et al.: Ozone-CO correlations determined by the TES satellite instrument  
in continental outflow regions, *Geophysical Research Letters*, Vol. 33(18),  
DOI:10.1029/2006gl026399, 2006.
- 1120 Zoogman, P., Jacob, D. J., et al.: "Improved monitoring of surface ozone by joint assimilation of  
geostationary satellite observations of ozone and CO." *Atmospheric Environment*, Vol. 84(0):  
p. 254-261. DOI:10.1016/j.atmosenv.2013.11.048, 2014.
- Zoogman, P., Liu, X., Suleiman, R.M., Pennington, W.F., Flittner, D.E., Al-Saadi, J. A., Hilton, B.  
B., Nicks, D. K., Newchurch, M. J., Carr, J. L., Janz, S. J., Andraschko, M.R., Arola, A., Baker,  
1125 B. D., Canova, B. P., Chan Miller, C., Cohen, R. C., Davis, J. E., Dussault, M. E., Edwards,



1130 D. P., Fishman, J., González Abad, G., Grutter, M., Herman, J. R., Houck, J., Jacob, D. J., Joiner, J., Kerridge, B. J., Kim, J., Krotkov, N. A., Lamsal, L., Lif, C., Lindfors, A., Martin, R. V., McElroy, C. T., McLinden, C., Natraj, V., Neil, D. O., Nowlan, C. R., O'Sullivan, E. J., Palmer, P. I., Pierce, R. B., Pippin, M. R., Saiz-Lopez, A., Spurr, R. J. D., Szykman, J. J., Torres, O., Veefkind, J. P., Veihelmann, B., Wang, H., Wang, J., Ghula, A., and Chance, K.: Tropospheric Emissions: Monitoring of Pollution (TEMPO), *J. Quant. Spectrosc. Radiat. Transfer.* 186, 17–39, doi:10.1016/j.jqsrt.2016.05.008, 2016.